

SESSION 16

OPEN END

Wednesday: July 27, 1994  
Co-Chairmen: M. W. First  
K. Duvall

OPENING COMMENTS OF SESSION CO-CHAIRMAN FIRST

BAR CODED AIR SAMPLE TRACKING: HOW IT CAN ASSIST IN  
COMPLIANCE WITH THE DOE'S NEW 10 CFR 835 AND THE NRC'S 10 CFR  
20 REGULATION

W. H. Bailey

EXPERIMENTAL STUDY OF ELEMENTARY COLLECTION EFFICIENCY OF  
AEROSOLS BY SPRAY: DESIGN OF THE EXPERIMENTAL DEVICE

D. Ducret, S. LeGarrec, J. Vendel

DEGRADATION OF HEPA FILTERS EXPOSED TO DMSO

W. Bergman, K. Wilson, G. Larsen, R. Lopez, J. LeMay

PROPOSED RETROFIT OF HEPA FILTER PLENUMS WITH INJECTION  
AND SAMPLING MANIFOLDS FOR IN-PLACE FILTER TESTING

J. K. Fretthold

**OPENING COMMENTS OF SESSION CO-CHAIRMAN FIRST**

Welcome to the session that we call "open end". This session follows a long tradition at the air cleaning conferences. The significance of the session is that it is a place for short presentations, for progress reports on research underway, for studies of operations that are in progress and that have already produced enough interesting significant information to make a progress report worthwhile. In addition to that, we encourage people who have problems of a puzzling nature to present them here and ask the assembled audience if there is somebody in the auditorium who might have had some experience or special knowledge that would be helpful in solving the problem. These are intended to be short presentations with a great deal of commentary following each one. This afternoon we have a number of presentations.

# 23rd DOE/NRC NUCLEAR AIR CLEANING AND TREATMENT CONFERENCE

## BAR CODED AIR SAMPLE TRACKING

### HOW IT CAN ASSIST IN COMPLIANCE WITH THE DOE'S NEW 10 CFR 835 AND THE NRC'S 10 CFR 20 REGULATION

W. Henry Bailey, Sales Manager  
NFS Radiation Protection Systems, Inc.  
Erwin, Tennessee 37650  
(615) 743-1779

#### 1.0 Introduction

With new government regulations on the horizon, advanced technology will become a necessity for the accurate assessment of air sampling data and maintaining internal dose ALARA. Bar coding is one advanced technology which has provided significant improvements in radiological air sample tracking and accountability. When combined with specific hardware and software, bar code technology can be used to automate procedures and enhance the data accuracy associated with air sampling in the workplace. This paper discusses some of the regulatory issues regarding radiological air sampling and describes how improved bar coded accountability techniques can assist in regulatory compliance.

#### 2.0 Air Sampling Regulations

Regulations specify that ambient air sampling be performed as a means of monitoring airborne radioactivity in and around work areas. Government regulations such as the Nuclear Regulatory Commission's (NRC) revised 10 CFR 20, the Department of Energy's (DOE) draft 10 CFR 835, and DOE Order 5480.11 state that occupational workers and the workplace be routinely monitored. Many facilities will need to modify their air sampling programs in order to comply with regulations.

#### 2.1 Revised NRC 10 CFR 20 Regulations

The main impact of the revised 10 CFR 20 (which is scheduled to be implemented on January 1, 1994) is a requirement for facilities to sum both internal and external exposure. This requirement is based on ICRP methodology which states the sum of the risks from a given radionuclide to an organ or tissue should not exceed the risk of exposing the whole body uniformly to 5 rems per year. Because the 10 CFR 20 revision includes a more detailed system of dose limitations, many licensees will need to gather more detailed information than presently collected in order to accurately perform dose assessment. This will greatly effect how many facilities will implement air sampling to monitor for the potential of internal exposure. The NRC currently has issued, for comment, a draft regulatory guide titled "Air Sampling In The Workplace" as one method for meeting certain survey and dose assessment requirements proposed in the revised 10 CFR 20, "Standards for Protection

## 23rd DOE/NRC NUCLEAR AIR CLEANING AND TREATMENT CONFERENCE

Against Radiation." This document suggests that air sampling can be used to:

- (1) Ensure effective radioactive material confinement,
- (2) Measure airborne radioactive material concentrations in the workplace,
- (3) Estimate worker intakes,
- (4) Determine posting requirements,
- (5) Determine protective equipment requirements,
- (6) Serve as an early warning for significantly elevated levels of airborne activity, and
- (7) Determine the time of an exposure incident, a requirement for interpretation of bioassay data.

"Air Sampling in the Workplace" suggests that the extent of air sampling provided should be based on accurately documented historical air sample data and bioassay results. If such data is not available or is inaccurate, potential intakes and concentrations should be estimated based on consideration of the following:

- (1) The quantity of radioactive material being handled,
- (2) The material's Annual Limit on Intake (ALI),
- (3) The release fraction of radioactive material (based on the material's physical form or use),
- (4) The type of material confinement, and
- (5) Other factors appropriate for the specific facility.

The need for accurately documented historical air sampling data will become more stringent upon implementation of the revised NRC and DOE regulations. Several basic components are needed in order to establish an accurate air sampling program. Draft Regulatory Guide DG-8003 "Air Sampling In The Workplace" discusses the basic aspects which must be considered in order to implement an effective air sampling program. These aspects include:

- (1) The type of air sampling which should be used,
- (2) The location of air samples,
- (3) Demonstration that air samples are representative of air breathed by workers,
- (4) Adjustments to Derived Air Concentrations (DAC),
- (5) Measurement of the volume of air sampled, and
- (6) Evaluation of air sampling data.<sup>1</sup>

### 2.2 DOE Order 5480.11 and Draft 10 CFR 835 Regulations

DOE Order 5480.11, "Radiation Protection for Occupational Workers", was implemented to establish radiation protection standards and program requirements for DOE and DOE contractor operations. Proposed draft regulations, titled 10 CFR 835, could replace DOE Order 5480.11 in the near future. As currently written, the proposed 10 CFR 835 is very similar to the revised NRC 10 CFR 20 regulations in all aspects including air sampling.

## 23rd DOE/NRC NUCLEAR AIR CLEANING AND TREATMENT CONFERENCE

The proposed rule would require occupational workers and the workplace to be routinely monitored. Retrospective monitoring will be required in areas where workers are likely to exceed an annual intake of 2% (or more) of the ALI. In addition, real-time monitoring will be required in areas where workers are likely to be exposed to concentrations exceeding 10% of DAC.

Monitoring of individuals and areas should be performed to:

- (1) Demonstrate compliance with the regulations,
- (2) Document radiological conditions in the workplace,
- (3) Detect changes in radiological conditions,
- (4) Detect the gradual buildup of radioactive materials in the workplace,
- (5) Verify the effectiveness of engineering and process controls, and
- (6) Reduce radiation exposure.

In the event of upset conditions, analysis of data obtained from representative air sampling can be used to alert health physics personnel to possible internal exposure of an individual from the intake of radioactive material. Actual intake can then be measured using whole body counting and/or other bioassay techniques, as appropriate. According to the new rule, estimations of internal dose equivalent shall be based on bioassay data rather than air concentration values. However, air concentration values may be used for estimating internal dose if bioassay data is unavailable or inadequate.<sup>2</sup>

### 3.0 Effects of Regulations on Air Sampling Information Systems

New NRC and DOE requirements will likely effect air sampling information systems in many ways. Because many radionuclide airborne limits will be dramatically reduced by new regulations, additional data may be required in order to more accurately assess worker exposure. In addition, analysis trending and quality control methods may also be effected.

#### 3.1 Data Requirements for Air Sampling

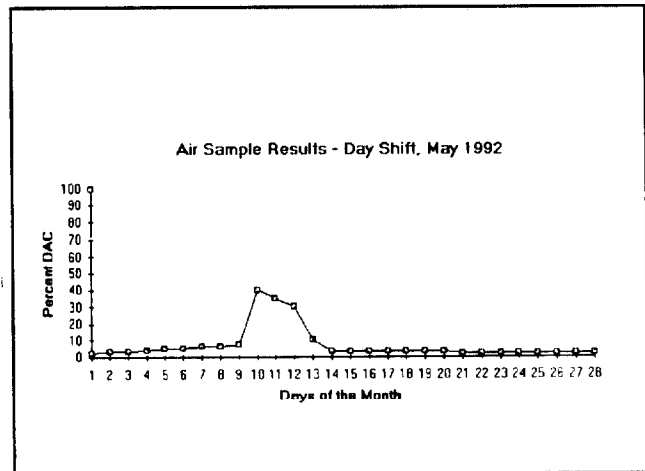
Proposed air sampling regulations could increase the amount of data required for air sampling due to the need to record additional information, such as particle size information, lung solubility studies, and air-flow rate correction calculations. Facilities which deal with alpha emitting radionuclides such as uranium and thorium will be most effected.

Without controls, as the amount of information gathered increases, so does the potential for more errors associated with air sample data collection. It is estimated that a facility which maintains and analyzes 100 area sampling locations and 20 lapel

samples at a rate of three shifts per day will require approximately 100 megabytes of annual computer storage for associated air sample data.<sup>3</sup>

### 3.2 Air Sample Analysis Trending and Quality Control

Air sample data can be used for analysis trending and quality control charts. This is highly desirable for demonstrating an effective ALARA program. These analysis functions can be easily communicated by charts and graphs which show air sampling results for various locations over a period of time. Analysis trending is also particularly useful when analyzed with respect to individual stations, areas, or buildings and associated activities performed during a specified period of time.



### 3.3 Accurate Record Keeping

A quality control method to ensure more accurate record keeping for air sampling begins by linking each sample filter to the sampling location. Without a high degree of confidence that air sample accountability is maintained, data regarding air sample locations should not be considered representative. For this reason, many licensees are evaluating new ways to collect data to insure a high degree of air sampling accountability.

## 4.0 Data Collection with Bar Codes

Bar codes offer one of the most accurate methods for data collection within the workplace. Air sample data collection can be greatly improved by implementing bar codes as a method of automatic identification. Through the bar coding of air sample filters, sampling locations, and personnel badges, technicians can use portable bar code readers to quickly and accurately collect air sample filters and corresponding data. Data entry using bar codes is one million times more accurate than manual key punch entry.<sup>4</sup> Therefore, air sample records created through use of bar codes ensures greater accuracy and reliability.

### 4.1 Bar Code Techniques

There are many types of bar coding formats (called symbologies)

available today. Depending upon the application or industry, a specific symbology is often required. For example, the retail industry standardized on the Universal Product Code (UPC) symbology. Some symbologies are designed for specific applications, such as Interleaved 2 of 5, which only contains numeric data.

For air sampling, symbology Code 3 of 9 (CODE 39) is recommended. The CODE 39 format is capable of handling the full range of alpha and numeric data and includes self checking characters built into the code itself. These capabilities provide a wide variety of air sample identification and error checking features to ensure better data accuracy and sample accountability.

### 4.2 Portable Bar Code Readers

Devices for reading bar codes are becoming smaller and smaller. Presently, a bar code decoder integrated into a powerful computer can be carried in the palm of the hand. These machines are capable of storing over one million bytes of information in non-volatile memory. Some models even contain fixed disk drives.

Sophisticated programs can turn these portable readers into devices which promote "Automated Procedures". Automated procedures refer to advances in portable bar code reader software which allows only valid data to be collected in the proper procedural sequence. Most portable readers contain a full keyboard, a 40- to 80-character display, an audible speaker, and enough battery power to collect data for an eight-hour period. Bar code scanning devices, such as lasers, can be integrated into portable bar code readers. In addition, most units can support external scanning devices such as wand scanners.

## 5.0 Implementing Bar Codes for Air Sampling

By implementing bar codes for air sampling, technicians can utilize the portable bar code reader to automatically perform many operations. For example, each air sample station can be checked for activation and to ensure that technicians perform proper procedures when bar codes are scanned. In addition, the portable reader can be used to automatically record the time and date of sample installation and collection via an internal clock.

### 5.1 General Air Sampling

By using specialized software operating on a personal computer, technicians can store data about each sampling area. This data can then be uploaded to the portable bar code reader. When linked with RWP's or personnel access records, general air sample information can be used to monitor for elevated airborne activity and to determine the need for bioassay analysis.

## 5.2 Representative Air Sampling

Specialized software and bar coding can also be used to provide dose estimates from stationary representative air samplers. When linked with a "time-in-area" system, Health Physics personnel can estimate an individual's internal exposure by correlating the air sample results with the time-in-area records. By bar coding the location at each workstation, each worker can scan their bar coded identification badge or card to record the time spent at each specific workstation. Air sample collection and analysis data can then be linked to each individual to assist with representative breathing zone sampling.

Lapel samples, another form of representative air sampling, can also be tracked using bar codes. In this case, the individual can be issued a bar coded identification such as a badge or card. Portable sampling pumps are bar coded to provide a more accurate record of lapel sampling activities. Portable bar code readers are used to obtain lapel sample information such as an individual's identification and lapel sample pump number. PC software can be utilized to download lapel sampling information.

## 5.3 Early Warning Air Samplers

Early warning samplers perform two functions simultaneously. They provide general area sampling while warning workers in the area of elevated airborne activity. Early warning air samples are collected in the same manner as general area samples and can be used to determine the need for bioassay analysis.

## 5.4 Tracking Air Sample Media

Tracking of air sampling media can be performed using several bar coding methods. These methods consist of applying bar codes to storage envelopes or attaching bar codes to the filter media itself. These methods have been found to be highly effective when combined with specialized PC software and portable bar code readers. By using software which operates on a microcomputer, technicians can eliminate the vast majority of manual data entry required for collecting air samples.

### 5.4.1 Bar Coded Envelopes

One of the easiest ways to improve air sample accountability is to directly apply bar coded labels to an air sample collection container such as an envelope. Portable bar code readers (loaded with special software) speed air sample collection. Bar code readers can be used to prompt technicians to scan an individual air sample location bar code and enter the ending vacuum flow rate. Technicians can then be prompted to remove the air sample filter, scan the corresponding envelope bar code and place the filter into the envelope. This operation links the air sample filter to the air sample location and the portable reader automatically records the time and date of sample collection. Technicians are prompted

by the bar code reader to place a new filter on the air sample station and adjust the beginning flow rate as instructed by the portable reader. Portable reader data is then downloaded to a microcomputer where it is merged with analysis data for reports and graphs.

### 5.4.2 Quick-Disconnects

Another method similar to bar coded envelopes involves quick-disconnect filter holders. Each filter holder is bar coded and equipped with a special fitting which allows the technician to quickly remove the entire air sample holder unit. This allows the air sample filter to be contained within the filter holder until it is brought back to the lab for analysis. This method works well for decommissioning projects and maintenance activities of short duration where the number of samples is small. By using portable bar code readers, bar coded air sample locations, and quick disconnect holders, technicians can improve sample accountability.

Portable readers prompt the technician to remove the air sample filter holder, scan the bar code and install the new holder and sample. As with the bar coded envelope method, the portable reader automatically records the time and date of sample collection and prompts the technician to adjust beginning flow rates for eventual flow rate averaging. Portable reader data is then downloaded to a microcomputer where it is merged with analysis data for reports and graphs.

### 5.4.3 Filter Cards

The previous two methods for tracking air sample filter media are very effective for tracking sample filters from the field to the lab for analysis. However, once in the lab, separating the sample media from it's identification in order to perform analysis is a weak link in the accountability chain. One way to ensure complete accountability throughout the sampling and analysis process is to bar code the sample itself. Placing a bar code label directly on the sample media will restrict the air flow through the filter. Therefore, bar coded filter cards are normally used to address the accountability issue. The filter media is held in place by special adhesives and uniquely numbered bar codes are printed on each card.

Portable readers prompt the technician to scan the air sample location bar code and enter the ending vacuum flow rate as previously discussed. Technicians are then prompted to remove the air sample filter card, scan the bar code located on the card and place the card in a protective envelope. This operation ensures that the correct filter card is linked to the air sample location.

Next, the portable reader prompts the technician to scan and install a new bar coded filter card. By doing so, the technician links the unique filter card with the sample location for complete

accountability throughout the sampling and analysis process. As with the bar coded envelopes and the quick disconnect holders, the portable reader automatically records the time and date of sample collection and prompts the technician to adjust beginning flow rates for flow rate averaging. Portable reader data is then downloaded to a microcomputer where it is merged with analysis data for reports and graphs. Bar code scanners mounted on analysis equipment can be used to read each sample as it is counted, so as to link the results with the sample identification.

#### 5.4.4 Adhesive Cards

Another device similar to the filter card is a bar coded adhesive card designed for lapel, early warning, and other air sample applications where the special filter holders needed for the filter card cannot currently be installed. This device allows technicians to place filter media onto an exposed adhesive area located in the center of the card.

Portable readers prompt the technician to scan the air sample location bar code and enter the ending vacuum flow rate as previously discussed. Technicians are then prompted to remove the air sample media, place the media on the adhesive card, scan the bar code located on the card and place the card in a protective envelope. This operation ensures that the correct filter card is linked to the air sample location.

Next, the portable reader prompts the technician to scan and install a new air sample filter. As with the bar coded filter cards, the portable reader automatically records the time and date of sample collection and prompts the technician to adjust beginning flow rates for flow rate averaging. Portable reader data is then downloaded to a microcomputer where it is merged with analysis data for reports and graphs. As with the bar coded filter card, analysis equipment containing a bar code scanner can read each sample as it is counted, so as to link the results with the sample identification.

### 6.0 Case Studies

Many DOE and NRC licensed facilities have implemented one or more of the bar coded air sampling techniques discussed above. Improved data accuracy, along with rapid analysis results were the main reasons for implementing a bar code air sampling system. However, these facilities also received the added benefit of substantial cost savings and improved worker efficiency through implementation of bar coded air sampling programs. The following represents case studies of four such facilities.

#### 6.1 DOE Uranium Materials Facility

A uranium materials facility implemented a bar coded air sample tracking system in 1991 to track approximately 50 general area air

## 23rd DOE/NRC NUCLEAR AIR CLEANING AND TREATMENT CONFERENCE

samples utilizing a bar coded envelope method. The purpose of the system was to address the following areas:

- 1) Provide better accountability for air samples,
- 2) Reduce errors associated with air sample collection, analysis, and reporting, and
- 3) Improve the efficiency associated with general area air sampling.

The facility utilizes an automatic, low-background, alpha/beta counter for air sample analysis. Portable bar code readers with hand-held laser scanners are used for air sample data collection. The portable readers are carried in protective cases which can be easily decontaminated. The portable readers contain software that helps to automate procedures and permits the air sample data to be downloaded to a microcomputer which merges analysis data with the bar code reader data to produce radioactive airborne concentration reports. The analysis data is also exported to the site's minicomputer to supplement personnel exposure data.

The bar coded air sampling system has allowed the uranium materials facility to increase the number of air samplers in use, while at the same time improving the accountability associated with air sample data. The site's bar coded system promotes standardized collection procedures and allows reporting of consistent, legally defensible air sample results regardless of the technician performing the work.

Site personnel estimate that the bar coded air sample tracking system has significantly improved air sample accountability and reduced data entry errors by 75%. In addition, microcomputer software designed for bar coded air sampling has reduced man-hour requirements for air sampling by 40%. Man-power previously allocated for data entry is now being used to perform a greater amount of data analysis and corrective actions, thus lowering the potential risk to workers.

### 6.2 Plutonium Fuel Facility Decommissioning Project

A plutonium fuel facility decommissioning project implemented a bar coded air sampling system in 1990 to track approximately 30 general area air samples utilizing the quick-disconnect method. The purpose of the system is to address the following areas:

- 1) Provide better accountability for air samples,
- 2) Provide accurate data to ensure worker safety during decommissioning, and
- 3) Improve the efficiency associated with routine and non-routine air sampling.

The facility utilizes an automatic, low-background, alpha/beta counter for air sample analysis. Portable bar code readers with hand-held laser scanners are used for air sample data collection.

The portable readers contain software that helps to automate procedures and permits the air sample data to be downloaded to a microcomputer which merges analysis data with the bar code reader data to produce radioactive airborne concentration reports. The analysis data is also exported to the site mainframe computer to supplement personnel exposure data. To date, it is estimated that the bar coded air sample tracking system has maintained sample accountability and saved approximately 50% in man-hours when compared to manual data collection and reporting methods.

Bar coding has provided the decommissioning project with the capability to collect non-routine (as well as routine) air samples. For example, four or five samples may be non-routinely collected in a specific area to evaluate airborne radioactive conditions which may be elevated due to an increase in decommissioning activities. The data associated with the non-routine samples is also managed by the project's bar code tracking system. In addition, many glove box leaks were rapidly detected and repaired throughout the life of the 5-year project as a result of the speed associated with bar coded sampling systems.

### 6.3 Environmental Remediation Project

An environmental remediation project involving uranium contaminated sludge implemented a bar coded air sampling system in 1991 to track approximately 12 general area air samples utilizing the quick-disconnect method. The purpose of the system is to address the following areas:

- 1) Provide better accountability for air samples,
- 2) Provide accurate data to ensure worker safety during remediation, and
- 3) Improve the efficiency associated with routine and non-routine air sampling.

The facility utilizes an automatic, low-background, alpha/beta counter for air sample analysis and portable bar code readers with built-in laser scanners. The air sample collection and analysis methods are similar to those implemented for the decommissioning project described in Section 6.2 above. The analysis data is also exported to the site mainframe computer to supplement personnel exposure data. To date, it is estimated that the bar coded air sample tracking system has maintained sample accountability and saved approximately 25% in man-hours compared to manual data collection and reporting methods.

Bar coding has provided the remediation project with the capability to collect non-routine (as well as routine) air samples while maintaining data integrity. For example, three or four samples may be collected in a specific area to evaluate airborne radioactive conditions which may be elevated due to an increase caused by dewatering activities. The data associated with the non-routine samples is also managed by the bar code tracking system.

## 23rd DOE/NRC NUCLEAR AIR CLEANING AND TREATMENT CONFERENCE

### 6.4 NRC Licensed Uranium Fuel Facility

An NRC licensed uranium fuel facility implemented a bar coded air sampling system in 1987 to track approximately 250 representative air samples utilizing the bar coded filter card method. The purpose of the system is to address the following areas:

- 1) Provide very high accountability of air samples,
- 2) Ensure accurate data to ensure worker safety during fuel production, and
- 3) Provide efficient air sample collection for large number of air samples.

Because 250 air samples are collected each shift (750 per day), maintaining a high degree of sample accountability is very important. It is estimated that the bar coded air sample tracking system provides a 95% confidence level of air sample accountability and data accuracy. In addition, the man-hours saved by utilizing the system is estimated to be about 75% less than manual methods of data collection. An automated time and attendance system (also implemented at the facility) allows each worker's time-in area to be correlated with area air sample results to estimate worker exposure.

Automatic, alpha counters equipped with bar code scanners are used for air sample analysis. Portable bar code readers with wands are used for data collection. Special software loaded into the portable readers helps to automate air sampling procedures and provides the technicians with an efficient method for air sample collection. The software also permits air sample data to be downloaded to a microcomputer which merges analysis data with the bar code reader data to produce radioactive airborne concentration reports. The analysis data is exported to the site mainframe computer to be correlated with time and attendance data for personnel exposure tracking and air sample analysis trending.

### 7.0 Conclusion

New regulations will drive the need for more accurate and efficient data collection. Air sampling is an area where improved data accuracy and collection efficiency can increase worker safety. In addition, air sample accountability will become more important as internal exposure monitoring requirements become more stringent.

Case studies indicate that bar coded systems can greatly enhance air sample accountability, and enhance data accuracy. In addition, they can also promote timely review of data, promote analysis trending, and improve collection efficiency in the workplace. Man-power savings achieved through automation can be redirected towards a closer review of air sample results to ensure compliance with expected reductions in airborne activity limits.

References

- <sup>1</sup> "Regulatory Guide 8.25, Air Sampling in the Workplace", Regulatory Guide DG-8003, U.S. Nuclear Regulatory Commission, 1992.
- <sup>2</sup> "Department of Energy Proposed Primary Standards for Radiation Protection for Occupational Workers", Federal Register, Vol. 56, No. 236, 1991.
- <sup>3</sup> Data estimates based upon historical results obtained from case studies.
- <sup>4</sup> Allais, David C., "Bar Code Symbology", Intermec Corporation, May, 1985, Pg 1.

DISCUSSION

**FIRST:** Where did you come up with a million times less chance for error with bar codes than with manual tracking? Is this something quantitative or is it somebody's imagination?

**BAILEY:** It was obtained from the bar code symbology book published by Intermec Corporation.

**FIRST:** The people who supply the bar codes?

**BAILEY:** The people who supply the bar codes.

**FIRST:** It is certainly an unbiased source. Let me ask you a serious question. The examples you showed were for radioactive counting. How would the bar code work if you were going to take the filter off and weigh it by an electrobalance, because, practically, you could not weigh the card with the filter, or if you wanted to subject the sample to a chemical analysis? How do you have assurance that the bar code stays with the sample?

**BAILEY:** One of the ways that you can do this is by setting up a bar code scanner that links to the analysis equipment, such as a chemical analytical device, and then scanning the bar code at the time that the sample is removed from its holder and placed in solution.

*Experimental study of elementary collection efficiency of aerosols  
by spray : design of the experimental device*

D. DUCRET\*, S. LE GARREC\*\*, J. VENDEL\*

\* Institut de Protection et de Sûreté Nucléaire

Département de Protection de l'Environnement et des Installations  
Service d'Etudes et de Recherches en Aérocontamination et en Confinement  
IPSN/CEA - 91191 Gif-sur-Yvette Cédex FRANCE

\*\* Société des Techniques en Milieu Ionisant

Abstract

The safety of a nuclear power plant containment building, in which pressure and temperature could increase because of a overheating reactor accident, can be achieved by spraying water drops. The spray reduces the pressure and the temperature levels by condensation of steam on cold water drops. The more stringent thermodynamic conditions are a pressure of  $5 \cdot 10^5$  Pa (due to steam emission) and a temperature of 413 K. Moreover its energy dissipation function, the spray leads to the washout of fission product particles emitted in the reactor building atmosphere. The present study includes a large program devoted to the evaluation of realistic washout rates. The aim of this work is to develop experiments in order to determine the collection efficiency of aerosols by a single drop. To do this, the experimental device has to be designed with fundamental criteria :

- Thermodynamic conditions have to be representative of post-accident atmosphere.
- Thermodynamic equilibrium has to be attained between the water drops and the gaseous phase.
- Thermophoretic, diffusiophoretic and mechanical effects have to be studied independently.
- Operating conditions have to be homogenous and constant during each experiment.

This paper presents the design of the experimental device. In practice, the consequences on the design of each of the criteria given previously and the necessity of being representative of the real conditions will be described.

NOMENCLATURE

Particle characteristics:

Cu	: Cunningham slip-flow correction	(-)
$D_p$	: particle diameter	(m)
Kn	: Knudsen number	(-)
$k_p$	: thermal conductivity	(W.m <sup>-1</sup> .K <sup>-1</sup> )
Stk	: Stokes number	(-)
g	: gravity acceleration	(m.s <sup>-2</sup> )

Drop characteristics:

$Cp_d$	: specific heat	(J.kg <sup>-1</sup> .K <sup>-1</sup> )
$D_d$	: drop diameter	(m)
Heq	: equilibrium height	(m)
L	: heat of vaporization	(J.kg <sup>-1</sup> )
$m_d$	: drop mass	(kg)
$M_w$	: water molar mass	(kg)
Re	: Reynolds number	(-)
$T_d$	: drop temperature	(K)
$V_d$	: settling drop velocity	(m.s <sup>-1</sup> )
$\rho_d$	: drop density	(kg.m <sup>-3</sup> )

Gas characteristics:

$D_s$	: steam diffusivity	$(m^2.s^{-1})$
$k_F$	: thermal conductivity	$(W.m^{-1}.K^{-1})$
$M_a$	: dry air molar mass	$(kg)$
$M_s$	: steam molar mass	$(kg)$
$Pr$	: Prandtl number	$(-)$
$P$	: total pressure	$(Pa)$
$P_s$	: partial steam pressure	$(Pa)$
$P_{sv}$	: saturation vapor pressure	$(Pa)$
$R$	: molar gas constant	$(J.mol^{-1}.K^{-1})$
$S$	: saturation rate	$(-)$
$Sc$	: Schmidt number	$(-)$
$T_F$	: gas temperature	$(K)$
$X_a$	: dry gas fraction in moist gas	$(-)$
$X_s$	: steam fraction in moist gas	$(-)$
$\mu_F$	: gas viscosity	$(Pa.s)$
$\rho_{s,F}$	: density of steam in gas	$(kg.m^{-3})$
$\rho_{s,d}$	: density of steam in gas around drop	$(kg.m^{-3})$
$\rho_F$	: gas density	$(kg.m^{-3})$

**I. INTRODUCTION**

The safety of a nuclear power plant containment building can be achieved by spraying water drops. Severe accident scenarios (rupture of steam pipe or coolant system loss) provide for pressure and temperature increase. The spray reduces the pressure and the temperature levels inside the containment building by condensation of steam on cold water drops. The most stringent thermodynamic conditions are a pressure of  $5.10^5$  Pa and a temperature of 413 K in present reactors. In the future, these conditions will be  $7.7.10^5$  Pa and 433 K. Moreover its energy dissipation function, the spray leads to the washout of fission products emitted in the reactor building atmosphere. Safety studies show that the median diameter of aerosols in case of overheating accident would vary between 0.1 and 5  $\mu$ m. At present time, washout rates provide conservative assumptions in safety studies. This study includes a large program devoted to :

- . determine realistic washout rates for present reactor
- . optimize washout function of spray in futur reactor

The first step, which is the aim of this work, is to develop experiments in order to determine the collection efficiency of aerosols by falling drops in severe accident representative conditions.

**II. WASHOUT MECHANISMS**

Aerosols fission product washout results of mechanical and phoretic effects.

**Mechanical effects:** differential settling velocity between drops and aerosols induces collisions. There are three mechanical effects and their relative importances are function of drop and aerosol diameters.

► *impaction* : falling drop velocity induces fluid flow variations. High inertia particles turn off flow lines and then are collected on drops. This mechanism increases with drop velocity and particle diameter.

► *interception* : this mechanism is just a geometric effect and then independent of falling drop

velocity. This mechanism increases with  $\frac{D_p}{D_d}$  .

► *wake-capture* : small particles collection efficiency increases for drops which Reynolds numbers are between 30 and 300. Small particles, without significant inertia, trace the outline of drop and are collected in drop wake by eddy<sup>(1,2,3)</sup>. For Reynolds numbers larger than 300, collection efficiency decreases swiftly. So there is an optimum for  $Re \approx 300$ .

**Phoretic effects:** temperature and steam concentration gradients around drops induce aerosol collection by thermophoresis and diffusiophoresis.

► *Diffusiophoresis:* steam condensation on cold water drops induces molecular steam flow rate towards drops. This flow drags along particles. PRUPPACHER and KLETT<sup>(4)</sup> propose a theoretical collection efficiency :

$$E = \frac{C_D 2 M_a D_a (1 + \sigma_{s/a} \cdot X_a)}{D_d V_d \rho_F M_w} (\rho_{s,F} - \rho_{s,d})$$

with :

$$C_D = 1 + 0.108 (Sc^{1/3} Re^{1/2})^2 \text{ for } Sc^{1/3} Re^{1/2} < 1.4$$

$$C_D = 0.78 + 0.308 Sc^{1/3} Re^{1/2} \text{ for } Sc^{1/3} Re^{1/2} \geq 1.4$$

$$\text{and : } \sigma_{s/a} = \frac{M_w^{1/2} - M_a^{1/2}}{X_a M_w^{1/2} - X_a M_a^{1/2}}$$

Collection efficiency is proportional to local concentration gradient and independent of drop size. Diffusiophoresis effect is very important for small particles ( $D_p \leq 2 \mu\text{m}$ ) for which impaction is not significant and particularly for small drops ( $D_d \leq 180 \mu\text{m}$ ) because wake-capture doesn't exist.

► *Thermophoresis:* local temperature gradient around drops induces thermophoresis force. PRUPPACHER and KLETT<sup>(4)</sup> propose a theoretical collection efficiency :

$$E = \frac{C_T 2 C k_F}{D_d V_d P} (T_F - T_d)$$

$$\text{with } C = \frac{0.4 Cu (k_F + 2.5 k_p Kn)}{(1 + 3 Kn) (k_p + 2 k_F + 5 k_p Kn)}$$

and

$$C_T = 1 + 0.108 (\text{Pr}^{1/3} \text{Re}^{1/2})^2 \quad \text{for } \text{Pr}^{1/3} \text{Re}^{1/2} < 1.4$$

$$C_T = 0.78 + 0.308 \text{Pr}^{1/3} \text{Re}^{1/2} \quad \text{for } \text{Pr}^{1/3} \text{Re}^{1/2} \geq 1.4$$

Thermophoresis collection efficiency is proportional to temperature gradient and in inverse ratio to pressure. This efficiency decreases swiftly for larger drops.

All washout mechanisms and their possible coupling can be represented, for each drop, by an elementary collection coefficient. This coefficient is function of drops, aerosols and gaseous characteristics. We can see on figure 1 from PRUPPACHER and KLETT<sup>(5)</sup>, the evolution of this coefficient versus drop radius for several relative humidities. These theoretical and experimental results show a great variation of the collection coefficient (factor 100).

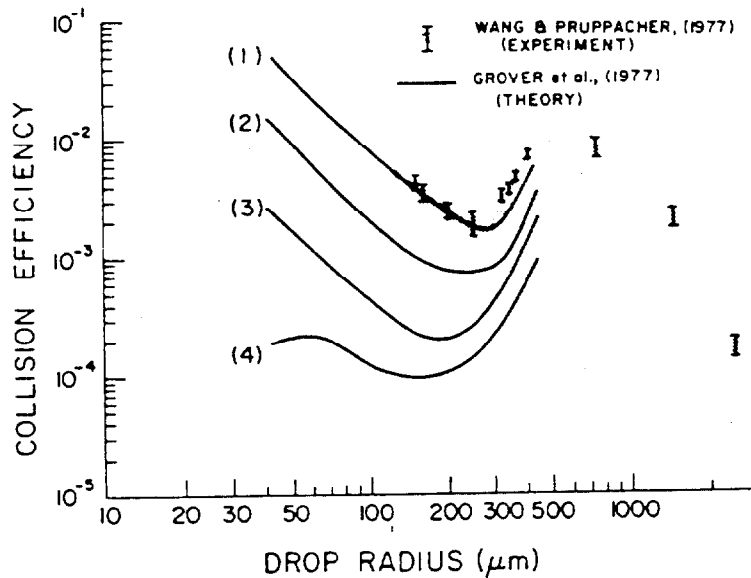


Figure 1 : Collision efficiency of particles ( $D_p = 0.5 \mu\text{m}$ ) as function of collection drop size for relative humidities of (1) 20 %, (2) 75 %, (3) 95 % and (4) 100 %

### III. DESIGN CRITERIA

There are theories and experiments but without specific thermodynamic conditions of spray system. So the experimental device is designed for a study of elementary collection coefficient in spray working conditions. The aim of this work is to develop analytical experiments to determine elementary collection coefficient of aerosols by a single drop. These results will be used to compute realistic washout rate of spray system.

To do this, the experimental device have to be designed with fundamental criteria :

► **Representative conditions:** in accident scenarios, with using spray system, thermodynamic conditions of reactor building atmosphere could change in a wide range. Moreover, prior results (figure 1) show a very large range of collection coefficient in function of different thermodynamic

conditions, aerosol and drop diameters. So experimental device would be able to reproduce the most of accident scenarios conditions.

► **Thermodynamic drop-gas equilibrium:** in order to determine precisely phoretic effects on collection, falling drop height must be enough for drops reach their thermodynamic drop-gas equilibrium. In fact, real equilibrium height is infinite. Moreover, phoretic effect is function of temperature gradient or steam concentration gradient, so we consider that equilibrium is reached when these gradients are insignificant. This equilibrium height is also very dependent of initial drop diameter. So we have determined experimentally drop size distribution of an industrial spray nozzle (SPRACO 1713A). Results (figure 2) show that drop diameters are in range from 20  $\mu\text{m}$  to 600  $\mu\text{m}$ , with a numeric median diameter of roughly 200  $\mu\text{m}$ .

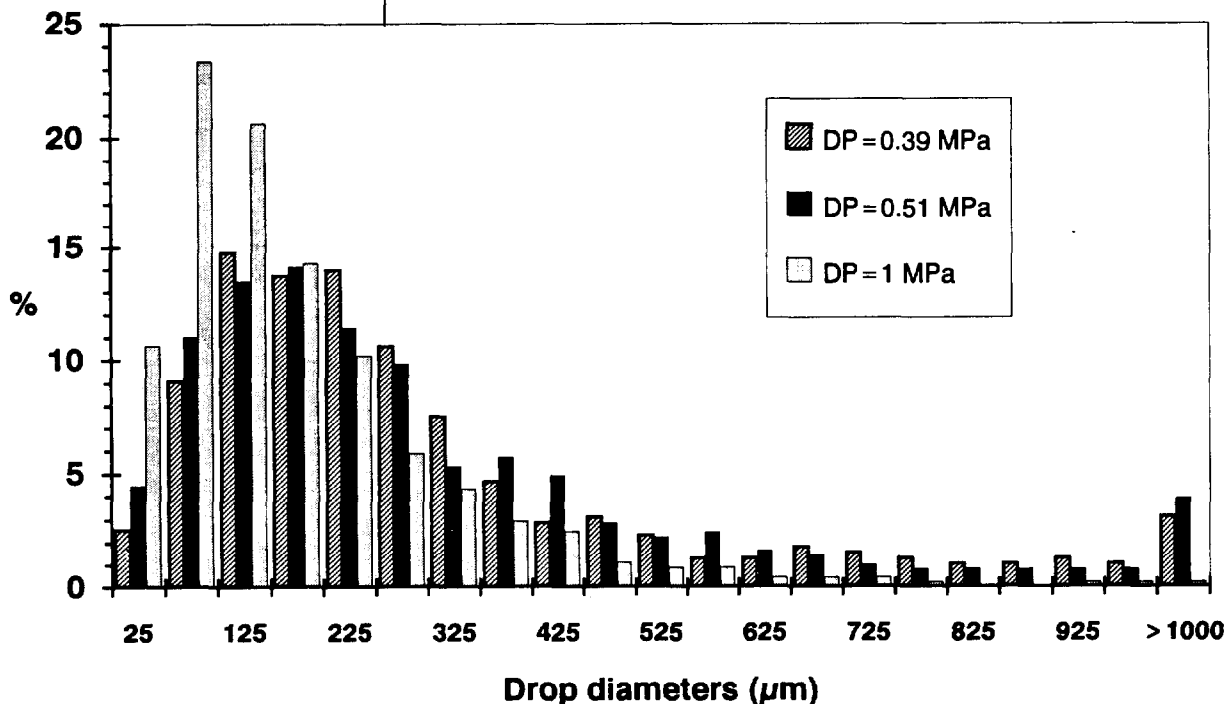


Figure 2 : Drop size distribution for different water pressures (DP)

► **Separate each washout mechanisms:** the study objective is to determine elementary collection efficiency of each effects independently. Then, experimental device must allow a great aptitude for different working conditions.

► **Steady-state and homogeneous working conditions:** the operating parameters are different from one experiment to an other, so as to represent all the spraying process conditions. But, in order to determine collection efficiency, we measure aerosol mass collected by drops, so during each experiment, these working conditions (pressure, temperature, saturation rate and aerosol concentration) have to be homogeneous and constant.

#### IV. DESIGN CRITERIA CONSEQUENCES

Experimental device is designed with these criteria:

► **Representative conditions:** from accident scenarios and calculation code, working conditions, which would be reproduce in experiments, are :

pressure : from  $10^5$  to  $5 \cdot 10^5$  Pa  
 temperature : from 293 to 413 K  
 steam saturation rate : from 0 to 1  
 aerosol diameters : from 0.1 to  $5 \mu\text{m}$   
 drop diameters : from 100 to  $500 \mu\text{m}$

Futur reactor conditions will be study, so experimental device is also designed for a pressure of  $7,7 \cdot 10^5$  Pa and a temperature of 433 K.

In order to separate each washout mechanism and to modelize, each working condition must be adjust inependently.

► **Thermodynamic drop-gas equilibrium:** steam mass transfert flow is proportional to local steam concentration gradient. We consider that equilibrium is reached when drop temperature is equal to fluid saturation temperature, taking into account the second decimal. For large drops ( $> 100 \mu\text{m}$ ) curvature effect of the drop surface on equilibrium vapor pressure is insignificant. So, kinetic condensation equations are :

drop diameter variation ( $dD_d$ ) during  $\Delta t$  :

$$dD_d = \frac{4 \cdot D_s \cdot M_s}{D_d \cdot \rho_d \cdot R} \left[ \frac{P_s}{T_F} - \frac{P_{so}}{T_d} \right] \Delta t$$

with :  $P_s = P_{sv}(T_F) \cdot S$  and  $P_{so} = P_{sv}(T_d)$

drop mass variation is ( $dm_d$ ) then :

$$dm_d = \frac{\pi}{6} \rho_d ((D_d + dD_d)^3 - D_d^3)$$

and thermal balance is :

$$m_d \cdot Cp_d \cdot T_d + dm_d \cdot L + 2\pi D_d k_F (T_F - T_d) \Delta t = (m_d + dm_d) Cp_d (T_d + dT_d)$$

Using numerical integration, we determine equilibrium height as function of initial drop diameter for more stringent thermodynamic conditions (figure 3).

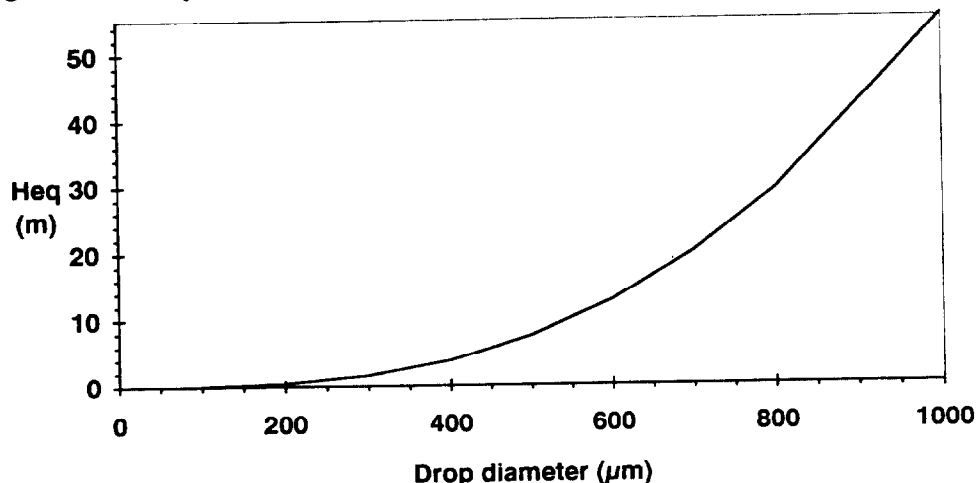


Figure 3: Equilibrium height as function of initial drop diameter  
 $P = 5 \cdot 10^5$  Pa,  $T_F = 413\text{K}$ ,  $S = 1$ ,  $T_d = 293$  K

Equilibrium height increases rapidly with initial drop diameter. But, in fact, phoretic effects are more important in the first falling meters. We can use the condensed water mass as equilibrium indicator. Equilibrium rate (EQUI), in function of drop position (y), is defined as :

$$\text{EQUI}(y) = \frac{D_d^3(y) - D_d^3(0)}{D_d^3(\text{Heq}) - D_d^3(0)}$$

(1-EQUI) represents the fraction of water which has not condensed after y meters of fall (figure 4).

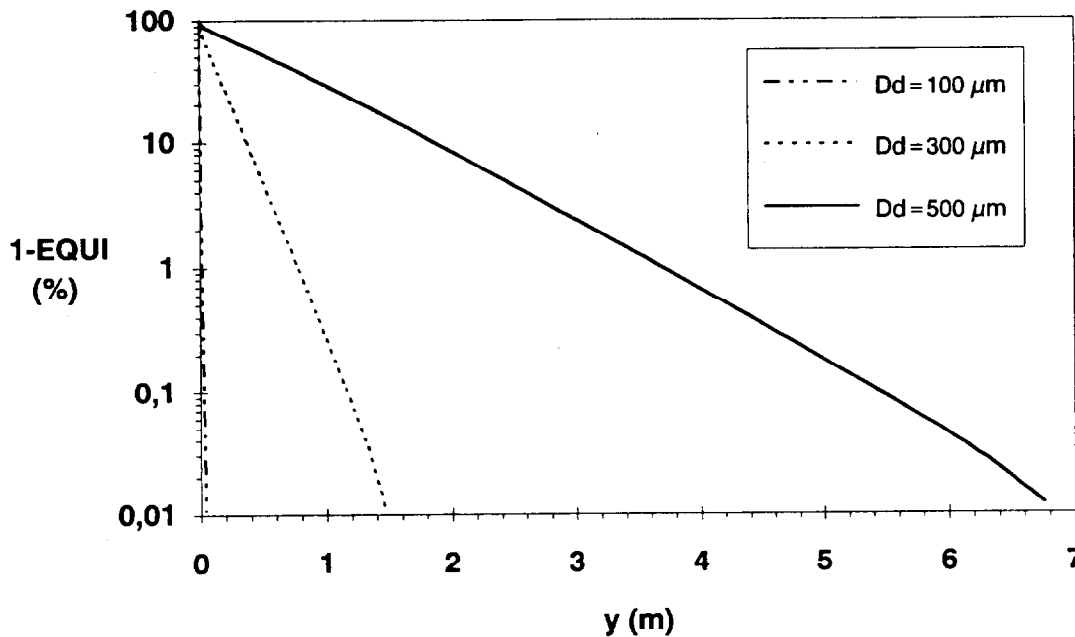


Figure 4: no condensed mass as function of falling height  
 $P = 5.10^5 \text{ Pa}$ ,  $T_F = 413 \text{ K}$ ,  $S = 1$ ,  $T_d = 293 \text{ K}$

For drop diameters ranging from 100 μm to 500 μm, a falling height of five meters is enough to condense more than 99 % of the water mass. So, we fixe our experimental device height at five meters.

► **Separate each washout mechanisms:** we have seen that with our experimental device each working conditions could be adjust independently and that phoretic effect can be study with a height of five meters. For mechanical effect determination, WANG and PRUPPACHER<sup>(4)</sup> advise that drop velocity is about 99 % of terminal settling velocity.

Basic dynamic equations of drop fall are :

$$m_d \frac{dV}{dt} = \frac{\pi}{6} D_d^3 (\rho_d - \rho_F) g - C_i \rho_F \frac{\pi}{8} D_d^2 V^2$$

Drag coefficient (C) is function of drop Reynolds number:

$$Re_d = \frac{\rho_F \cdot V \cdot D_d}{\mu_F}$$

for  $Re_d < 1 \Rightarrow C_t = \frac{24}{Re_d}$

for  $1 < Re_d < 905 \Rightarrow C_t = \frac{24}{Re_d} \left[ 1 + \frac{Re_d^{2/3}}{6} \right]$

for  $Re_d > 905 \Rightarrow C_t = 0,44$

terminal settling velocity ( $V_t$ ) is obtained for  $\frac{dV}{dt} = 0$

Drop velocity is computed by numeric integration :

$$V(t + \Delta t) = V(t) + \frac{dV}{dt} \Delta t$$

We can determine the drop fall height required for reach 99% of terminal velocity in function of drop diameter. For drop diameter of 500  $\mu m$ , these results (figure 5) show that without steam the height required is about 0.5 meter and with steam, this height is about two meters. In order to determine mechanical collection coefficient, a drop acceleration area without aerosol is needed. The height of this area is fixed at two meters.

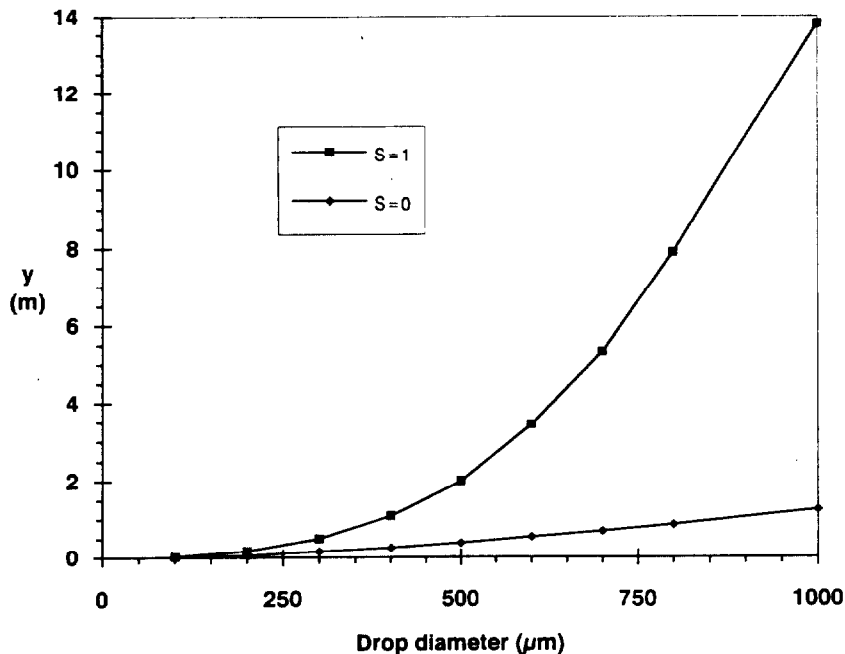


Figure 5: Falling height for reach 99% of  $V_t$  as function of drop diameter  
 $P = 5.10^5 Pa, T_F = 413 K, T_d = 293 K$

► **Steady-state and homogeneous working conditions:** homogeneity of working conditions (temperature and aerosol concentration) has been studied by numerical simulations of natural convection motion. The turbulence is modeled by using a  $k-\epsilon$  model in a code (TRIO-EF) developed in CEA. The simulations show that an efficient mixing can be achieved after 20 minutes by applying a temperature difference of only a few degrees between the walls and the bottom of the experimental enclosure (figure 6).

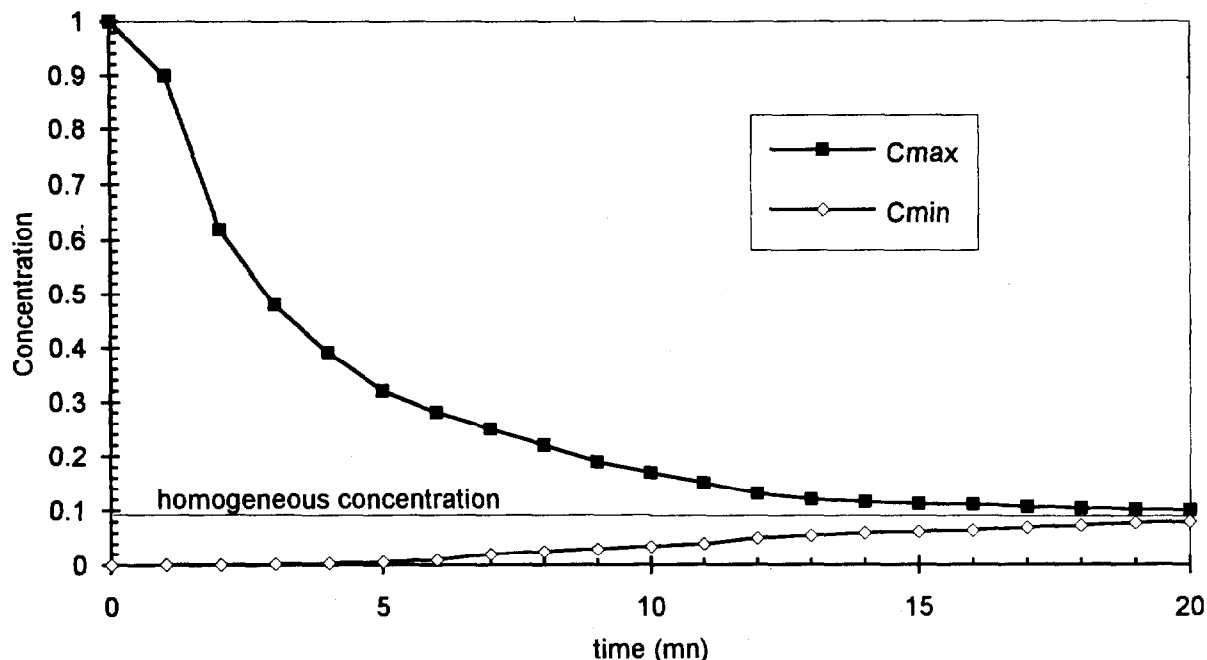


Figure 6: Evolution of maximal and minimal concentrations as a function of time

Several simulations, with a range of Grashof numbers between  $10^8$  and  $5 \cdot 10^{11}$  and a range of Prandtl numbers between 0.9 and 1.1, have been done in order to represent all possible thermodynamic working conditions.

Steady-state working conditions during each experiment is an important characteristic of this study. Using kinetic condensation equations, it is possible to compute steam volume removal by a drop. The most unsteady-state working conditions appear with an initial drop diameter of  $500 \mu\text{m}$ . In this case, each drop removes  $2 \cdot 10^{-8} \text{m}^3$  of steam. So, if we accept a pressure variation of 1 %, the number of drops injected in the device must be less than  $10^6$  drops. By using the greatest washout coefficient which can be expected (about  $10^{-1}$ ), the injection of  $10^6$  drops during an experiment induces a variation of aerosol concentration less than 7 %. Then we can consider a constant concentration.

## V. EXPERIMENTAL DEVICE DESCRIPTION

Using all design criteria described above, we have realized an experimental device.

The main characteristic is that these experiments will be analytic in order to modelize each collection mechanism in steady-state conditions. This concept induces short-time experiments and few drops injected.

The experimental device (figure 7) working conditions are :

- geometry: cylindrical
- drop falling height: 5 m
- enclosure diameter: 0.6 m
- temperature: from 293 K to 433 K
- total pressure: from  $10^5$  to  $8.10^5$  Pa
- steam saturation rate: from 0 to 1
- monodispersed drops diameter: from 100 to  $500 \mu\text{m}$
- aerosols aerodynamic diameter: from 0.1 to  $5 \mu\text{m}$
- aerosols nature: CsI

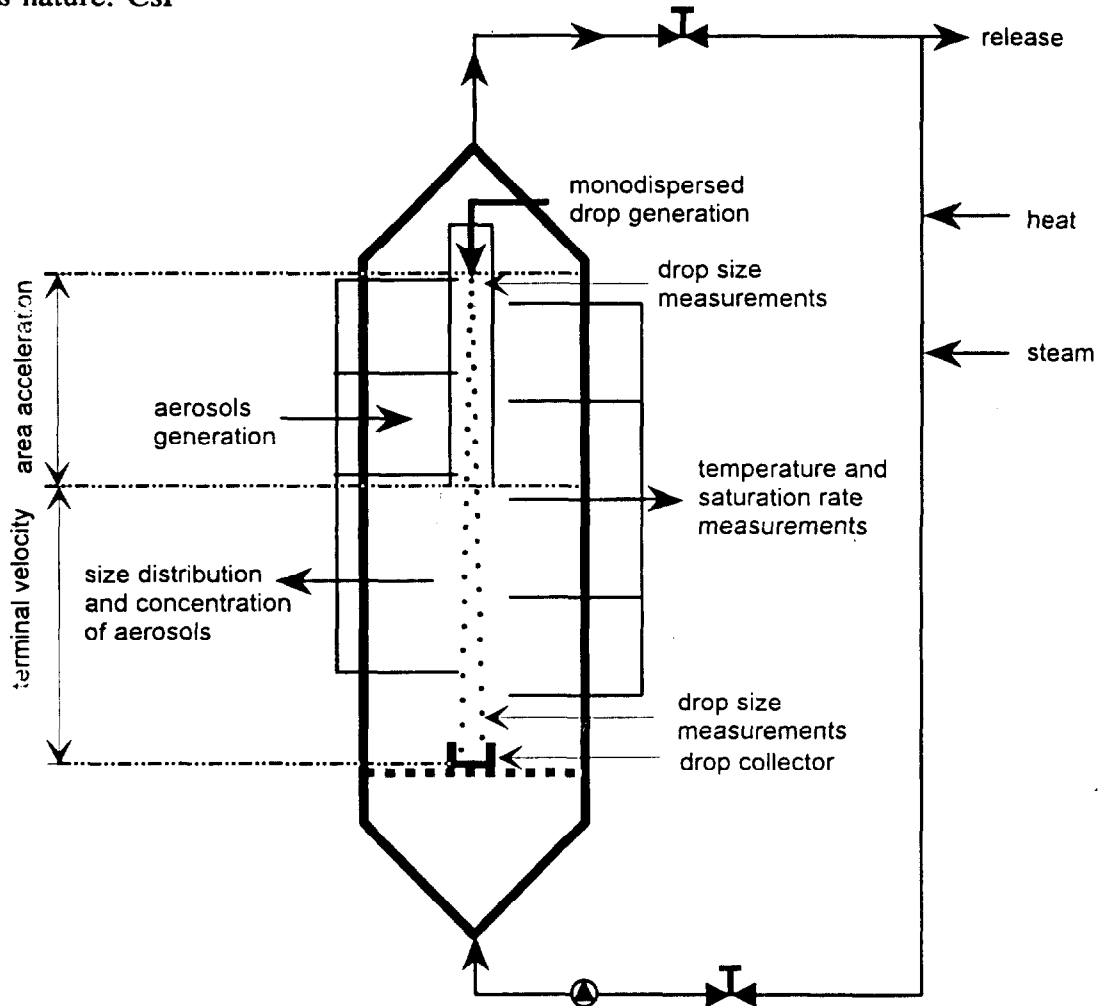


Figure 7: Scheme of experimental device

## VI. EXPERIMENTAL SET-UP

In order to determine the collection coefficient, each experiment, for fixed working conditions is in fact a succession of four tests. Experimental set up (figure 8) is based on the assumption that the different mechanisms are additive and independent.

**Test 1:** all washout mechanisms are taken into account. These test working conditions are representative of the experiment. Aerosol mass collected during this test is noted  $M_1$ .

## 23rd DOE/NRC NUCLEAR AIR CLEANING AND TREATMENT CONFERENCE

**Test 2:** only mechanical collection occurs during acceleration falling velocity and terminal velocity. Although thermodynamic conditions are different from test 1, mechanical effect parameters (viscosity and density) are comparable. Aerosol mass collected during this test is noted  $M_2$ .

**Test 3:** using acceleration area of drops in which there is no aerosol, we can determine mechanical collection with a constant velocity. Aerosol mass collected during this test is noted  $M_3$ .

**Test 4:** thermophoretic effect importance will be determined with this test. Steam saturation rate will be adjusted in order to have no evaporation. In fact, this collection effect will certainly be insignificant. Aerosol mass collected during this test is noted  $M_4$ .

By using aerosol mass collected by drops in each test, we can determine each collection effect :

- diffusiophoretic effect :  $M_1 - M_4$
- mechanical effect :  $M_3$
- thermophoretic effect :  $M_4 - M_2$

TEST NUMBER	1	2	3	4
washout mechanisms	mechanical diffusiophoresis thermophoresis	mechanical	mechanical with terminal settling velocity	mechanical thermophoresis
acceleration area	no	no	yes	no
$T_F$ (K)	413	293	293	413
P (Pa)	$5 \cdot 10^5$	$2.5 \cdot 10^5$	$2.5 \cdot 10^5$	$3.5 \cdot 10^5$
S (-)	0.95	$\approx 0$	$\approx 0$	$\approx 0$
$T_d$ (K)	293	293	293	293
$D_d$ ( $\mu\text{m}$ )	100 to 500 $\mu\text{m}$	100 to 500 $\mu\text{m}$	100 to 500 $\mu\text{m}$	100 to 500 $\mu\text{m}$
$\rho_F$ ( $\text{kg} \cdot \text{m}^{-3}$ )	3	3	3	3
$\mu_F$ (Pa.s)	$1.45 \cdot 10^{-5}$	$1.8 \cdot 10^{-5}$	$1.8 \cdot 10^{-5}$	$2.25 \cdot 10^{-5}$

Figure 8 : experimental set-up

CONCLUSIONS

This study, about design of the experimental device, shows the feasibility to determine experimentally collection coefficients of aerosols by falling drops. This experimental device, which is going to be realized, has two great specific characteristics:

- the most important is the concept of analytical experiments: we will measure elementary collection efficiencies of each collection mechanism,
- the second is that these experiments will be done with working conditions representative of nuclear power plant severe accident scenarios.

Using these experimental results, more accuracy washout rates will be computed in safety studies.

REFERENCES

- [1] BEARD K.V.  
Experimental and numerical collision efficiencies for sub-micron particles scavenged by small raindrops  
Journal of Atmospheric Sciences, vol. 33, 1595-1603, 1974
- [2] KERKER M. and HAMPL V.  
Scavenging of aerosol particles by a falling water drop and calculation of washout coefficients  
Journal of Atmospheric Sciences, vol. 31, 1368-1376, 1974
- [3] WANG P.K. and PRUPPACHER H.R.  
An experimental determination of the efficiency with which aerosol particles are collected by water drops in sub. saturated air  
Journal of Atmospheric Sciences, vol. 34, 1664-1669, 1977
- [4] PRUPPACHER H.R. and KLETT J.D.  
Microphysics of clouds and precipitation  
D. Reider Publishing C

DISCUSSION

**FIRST:** I had a question regarding the relevance of a 0.6 m tower in relation to a full-scale nuclear containment vessel. Have you taken scale into account? It is obvious that wall effects in a vessel of the diameter you used will have an important bearing on the final results. I am raising a question regarding the relevance of data in a 2 ft diameter cylinder to effects in a full-scale nuclear power plant containment vessel that will be perhaps 75-100 m in diameter. It would seem to me that a small vessel has important wall effects.

**DUCRET:** In this experiment we will analyze only the effects of drops without wall effects. The objective of this study is to measure only the collection by drops.

**SHER:** I have a related question. Is the experimental vessel completely filled with drops and completely filled with aerosol? Is there good mixing of the aerosol and droplet streams?

**DUCRET:** There is aerosol in the entire enclosure and a few drops are injected in the middle of the enclosure. Aerosol mixing will be achieved by natural motion and we will measure aerosol concentration in four samples. Because few drops will be injected, the aerosol and drop mixing will be good.

**SHER:** Do you have to worry about mixing of the aerosols with the drops?

**DUCRET:** It is a big problem but it is not the objective of the study. In our study, very few drops are injected so we assume a good mixing.

Degradation of HEPA Filters Exposed to DMSO\*  
by

W. Bergman, K. Wilson, G. Larsen, R. Lopez and J. LeMay  
Lawrence Livermore National Laboratory  
P.O. Box 5505, Livermore, CA 94550

Abstract

Dimethyl sulfoxide (DMSO) sprays are being used to remove the high explosive (HE) from nuclear weapons in the process of their dismantlement. A boxed 50 cfm HEPA filter with an integral prefilter was exposed to DMSO vapor and aerosols that were generated by a spray nozzle to simulate conditions expected in the HE dissolution operation. After 198 hours of operation, the pressure drop of the filter had increased from 1.15 inches to 2.85 inches, and the efficiency for 0.3  $\mu\text{m}$  dioctyl sebacate (DOS) aerosols decreased from 99.992% to 98.6%. Most of the DMSO aerosols had collected as a liquid pool inside the boxed HEPA. The liquid was blown out of the filter exit with 100 cfm air flow at the end of the test. Since the filter still met the minimum allowed efficiency of 99.97% after 166 hours of exposure, we recommend replacing the filter every 160 hours of operation or sooner if the pressure drop increases by 50%. Examination of the filter showed that visible cracks appeared at the joints of the wooden frame and a portion of the sealant had pulled away from the frame.

Since all of the DMSO will be trapped in the first HEPA filter, the second HEPA filter should not suffer from DMSO degradation. Thus the combined efficiency for the first filter (98.6%) and the second filter (99.97%) is 99.99996% for 0.3  $\mu\text{m}$  particles. If the first filter is replaced prior to its degradation, each of the filters will have 99.97% efficiency, and the combined efficiency will be 99.999991%. The collection efficiency for DMSO/HE aerosols will be much higher because the particle size is much greater.

---

\*This work was performed under the auspices of the U.S. Department of Energy by Lawrence Livermore National Laboratory under contract no. W-7405-eng.48.

## I. Introduction

This study was initiated in support of the nuclear weapons dismantlement program in which the HE, HMX, is being removed from the weapon by dissolution with DMSO. Heated DMSO is sprayed against the exposed HE to dissolve it and aid in breaking up the HE layer. The DMSO spray generates a high concentration of fine aerosols that is contained in a workstation. This aerosol may contain up to 25% by weight dissolved HE. The exhaust from the workstation is filtered through two, 135 cfm HEPA filters to prevent potential radioactive contamination or HE from being released to the environment.

A schematic of the ventilation system used for the HE dissolution workstation is shown in Figure 1. The ventilation system consists of a 35 cfm inlet HEPA filter with a butterfly valve to seal off the inlet during the DMSO spraying. The exhaust consists of two, 135 cfm HEPA filters in series followed by a Fischer valve (Associated Process Controls, Pleasanton, CA, 94566), and a flow meter. Although a standard 50 cfm HEPA filter would be sufficient to meet the required exhaust flow capacity of 55 cfm for safety considerations, we selected the 135 cfm HEPA filter to reduce the exhaust flow restrictions. The Fischer valve opens when the vacuum in the 16 cubic feet workstation drops below -1 inch of water and closes when the vacuum increases greater than -1 inch of water. During the dissolution process, there is no ventilation through the workstation except for short intervals when the Fischer valve opens to maintain a -1 inch of vacuum inside the workstation. After the dissolution operation is completed, the inlet butterfly valve is opened, and filtered room air sweeps the workstation clean and exhausts through the exhaust HEPA filter.

Since DMSO is an excellent solvent for many polymers, we were concerned that the solvent would dissolve the components of the HEPA filter and degrade the filter performance. The primary components of the HEPA filter that we suspected as being susceptible to attack from DMSO are the acrylic binder that holds the glass fibers together in the media and the polyurethane foam sealant that seals the pleated filter pack into the frame. The filter type that we tested was a combined, prefilter-HEPA filter unit boxed in a single plywood housing: Flanders, Dual Pack, 50 cfm, model 007-C-04-00-NL. The prefilter medium was a glass fiber medium with an atmospheric dust spot efficiency of 60% according to ASHRAE Standard 52-76. The HEPA medium met the requirements in MIL-F-51079.

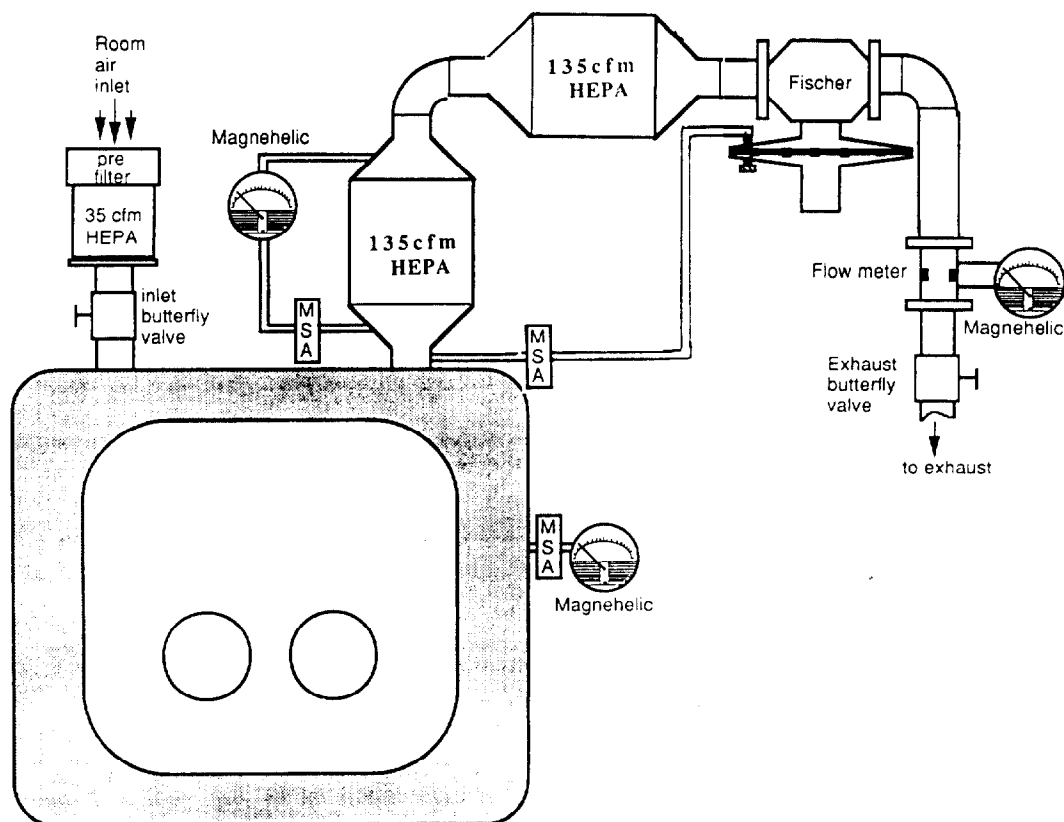


Figure 1. Ventilation system for the HE dissolution workstation.

## II. Characterizing DMSO challenge to HEPA filters

In order to evaluate the effect of the DMSO exposure on HEPA filters, we first had to characterize the challenge to the filters. Although the challenge consisted of both DMSO vapor and aerosols, we only measured the aerosol component. Since the spray operation generates a high concentration of aerosols, we could assume that the vapor concentration would be the saturated concentration, which is easily computed for each temperature. Table 1 shows the saturated vapor pressure and concentration of DMSO at various temperatures. Two of the data sets are experimental measurements, while the remainder were computed using the Clapeyron-Clausius equation

Table 1 Saturated DMSO vapor pressure and concentration

Temperature		Vapor Pressure	Concentration	
°F	°K	Torr	%	g/m <sup>3</sup>
72*	293	0.40*	0.05	1.7
100	311	1.39	0.18	5.3
122*	323	3.00*	0.39	11.7
150	339	7.43	0.98	27.6
189	360	22.8	3.00	79.5

\*experimental data

We measured the concentration and size distribution of the DMSO aerosols produced under simulated operating conditions using the apparatus shown in Figure 2.

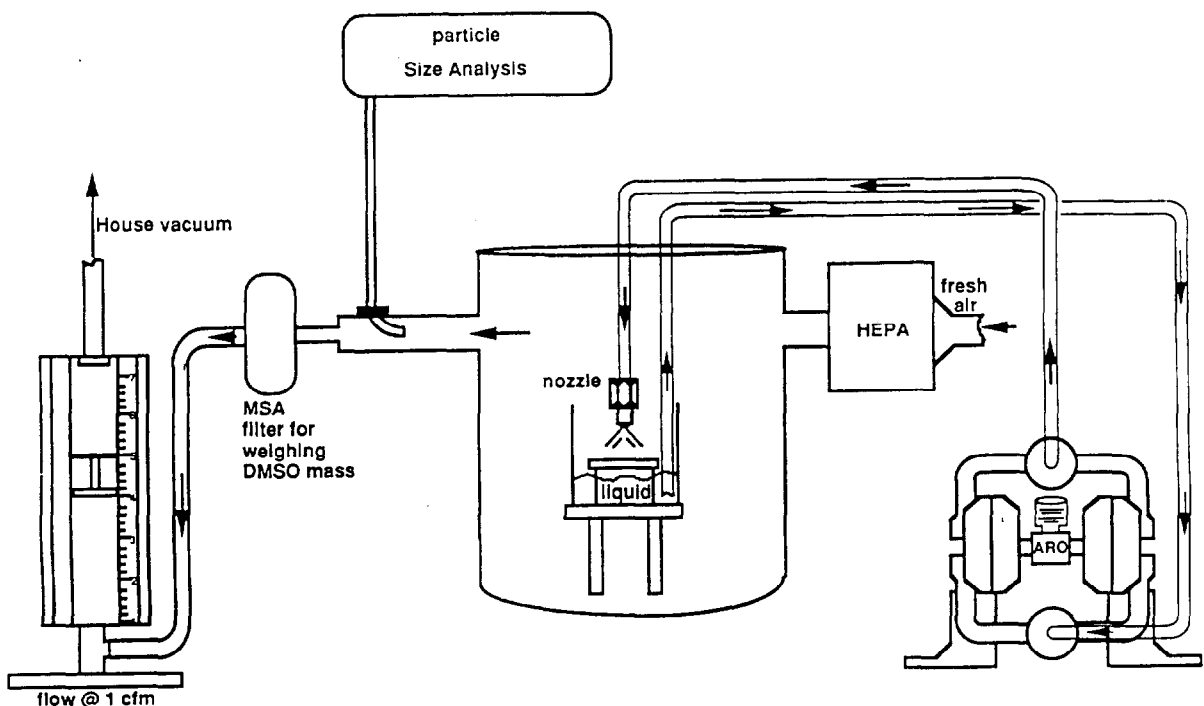


Figure 2. Experimental apparatus used for measuring the mass concentration and size distribution of DMSO aerosols generated from a single nozzle.

We simulated the work station and spray operation with a sealed Plexiglass chamber (0.87 cu. ft.) in which a spray nozzle was positioned 1.5 inches from a flat plate. In practice, multiple nozzles would be directed against the exposed HE. A piston pump (ARO) fed liquid DMSO at 100 psi to the spray nozzle and pulled liquid from a can that served both as a collector for the liquid run-off and as a reservoir. The temperature in the test chamber was at room temperature, about 70°F. The Plexiglass chamber also had a HEPA filtered inlet and a vacuum exhaust to simulate the ventilation system. We used a MSA respirator cartridge filter to filter the DMSO aerosols from the exhaust. The mass concentration of DMSO aerosols was determined by weighing the filter before and after the test and dividing by the air flow volume. The average concentration for four measurements is 3.3 g/m<sup>3</sup> with a standard deviation of ± 1.1 g/m<sup>3</sup>. We also measured the aerosol size distribution with a Climet 208 particle counter. Figure 3 shows the size distribution of DMSO aerosols plotted as a function of particle diameter. The peak number concentration occurs at 1.6 μm diameter.

- Background (counts/cc.-Log Width)
- Upstream (counts/cc.-Log Width)

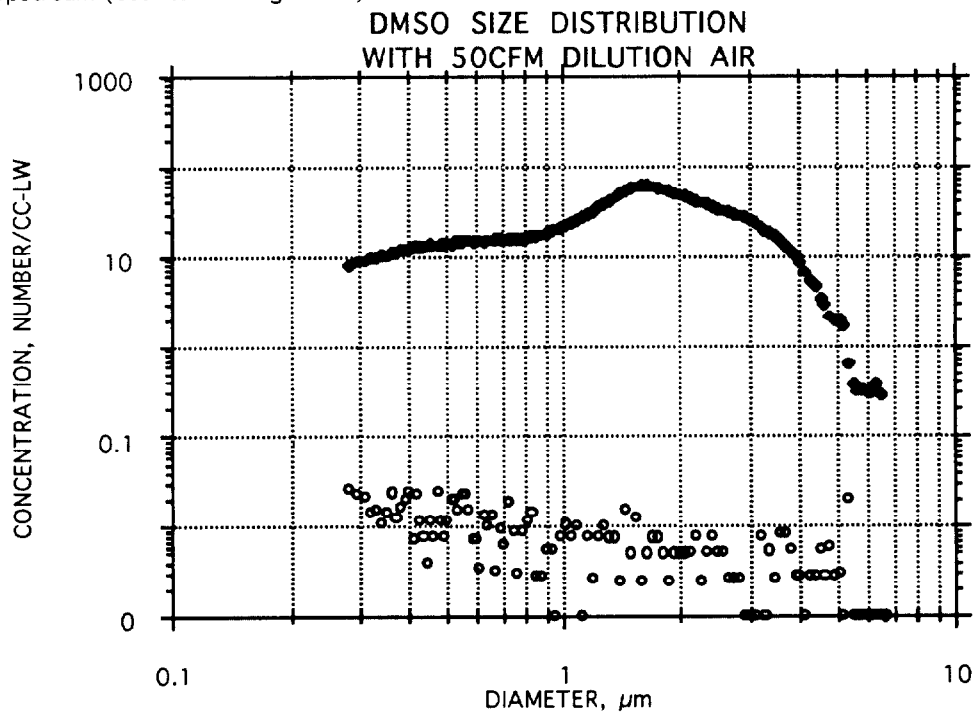


Figure 3. Size distribution of DMSO aerosols.

To verify that the DMSO concentration used in our filter experiments was realistic, we measured the mass concentration of DMSO/HE in a full-scale dissolution test. The tests were conducted on a simulated warhead that was sprayed with a solution of DMSO/HE. The temperature within the workstation was 120°F. Thirty-two nozzles ( 12 jets and 20 fans) were used in a manifold spray fixture. The aerosol mass was determined at twelve positions within a workstation that was 46 inches long, 34 inches wide, and 32 inches high.

Figure 4 shows a schematic of the workstation and sampling train used in the measurements along with the location of the twelve sampling locations. Each of the twelve sampling locations was six inches from the nearest wall. For example the top corner samples were taken six inches from the top wall and six inches from each side wall. The side samples were taken in the middle of the side wall, six inches from the side wall, and six inches from either the top or bottom walls. The aerosols were sampled at 1 cfm (0.0283 m<sup>3</sup>/min) for three minutes through eight feet of 0.625 inch ID nylon tubing prior to collection on a 2 inch filter disk that was cut from a standard HEPA media. The aerosol mass was determined by weighing the filter disks before and after the sample. No tests were conducted to establish the particle line loss since potential losses would be negligible compared to the variation in concentration found in the box. The concentration measurements were computed from the DMSO/HE mass collected divided by 0.0849 m<sup>3</sup> (0.0283 m<sup>3</sup>/min x 3 min.= 0.0849 m<sup>3</sup>) and are tabulated in Table 2.

The average DMSO/HE concentration from Table 2 is 1.87 g/m<sup>3</sup> with a standard deviation of  $\pm 0.57$  g/m<sup>3</sup>. This concentration is less than what was measured with a single nozzle in the apparatus shown in Figure 2. We suspect that the larger particles were quickly settling out in the workstation yielding a smaller average particle size and hence a lower mass concentration. The larger aerosols in the single nozzle apparatus could not settle out because all of the air was being swept out and filtered for mass determinations. In contrast there was no air flow in the workstation during the spraying operation to prevent the larger particles from settling out. We did not measure the aerosol size distribution in the workstation to confirm our hypothesis because our instruments would be contaminated with HE and could not be cleaned. However, during the purge cycle the large particles will also be swept out into the filtration system. Thus, the single nozzle measurements provide a more conservative measurement of aerosol mass concentration.



In addition to the DMSO aerosol challenge, the HEPA filters would also be exposed to a vapor challenge. As seen in Table 1, the vapor concentration is comparable to the aerosol challenge. At higher temperatures, the vapor concentration is much higher than the aerosol concentration. However, most of the vapor DMSO will pass through the HEPA filter whereas more than 99.97% of the DMSO aerosols will be trapped on the first HEPA filter. In practice, since the DMSO/HE particles are greater than 1  $\mu\text{m}$  diameter, more than 99.9999% of the DMSO/HE particles will be trapped on the first filter. Although we have not measured the size distribution of DMSO/HE aerosols, the dissolved HE should not significantly affect the size distribution. Thus based on the single nozzle and full-scale tests, we estimate that about 3  $\text{g}/\text{m}^3$  of aerosol and 1.7 to 35  $\text{g}/\text{m}^3$  of vapor will be generated in the DMSO workstation depending on the temperature between 72 F and 160 F. This aerosol and vapor will challenge the exhaust HEPA filter. At the higher temperature, a significant fraction of the DMSO vapor will penetrate the first filter and condense on the second filter.

Table 2 Concentration of DMSO aerosols at various locations in a HE dissolution workstation.

Location	Concentration $\text{g}/\text{m}^3$
Top Corner	
A	1.79
C	2.89
H	1.24
J	2.04
Bottom Corner	
B	1.62
D	2.76
I	1.31
K	1.58
Top Side	
E	1.30
G	2.48
Bottom Side	
F	2.16
L	1.41

### III. Filter Media Tests

We exposed samples of HEPA media cut from a new HEPA filter (MSA 50 cfm, part 464891) to saturated DMSO vapor and then conducted tensile strength tests on the exposed media. The precut media samples were suspended over a pool of DMSO contained in a sealed container. Since DMSO readily absorbs water, the samples were preconditioned at 50 C in a vacuum oven for 65 hours to remove any water absorbed on the media. We also conducted baseline tests on samples with and without preconditioning. The tensile strengths were measured using an Instron tester in both the machine direction (MD) and in the cross direction (CD). The results of our tests are shown in Table 3. The number of samples tested at each condition are shown in the table and provide a measure of the standard deviation.

Table 3 Media tensile strength after DMSO vapor exposure

Exposure	Pretest Conditioning	Maximum tensile load at failure (lbs)	
		Machine direction	Cross direction
Baseline (ambient air)	As-is	1.03±0.08	0.74±0.06
"	Dried under vac @ 50°C for 65 hrs	1.48±0.01	0.99±0.09
"	Dried under vac @ 50°C for 65 hrs	1.30±0.11	0.92±0.20
Sat'd DMSO vapor @ RT for 483 hours	Dried under vac @ 50°C for 43 hrs	1.32±0.04	0.99
Sat'd DMSO vapor @ 50°C for 343 hrs + 149 hrs @ RT	Dried under vac @ 50°C for 43 hrs	1.38±0.05	1.04

Note: The "±" values represent a single standard deviation.

The test results show that exposure to saturated DMSO vapor has no effect on the HEPA media strength. Table 3 also shows that the preconditioning increases the media strength by about 30%. We suspect that the pretreatment provided additional curing of the acrylic binder used to hold the fibers together in the media.

#### IV Filter Tests

We conducted a series of DMSO exposure tests on a boxed 50 cfm HEPA filter with an integral prefilter. This is the typical first stage filter used in the exhaust from glove boxes at LLNL. A photograph of the HEPA filter with flanges removed after the exposure test is shown in Figure 5.

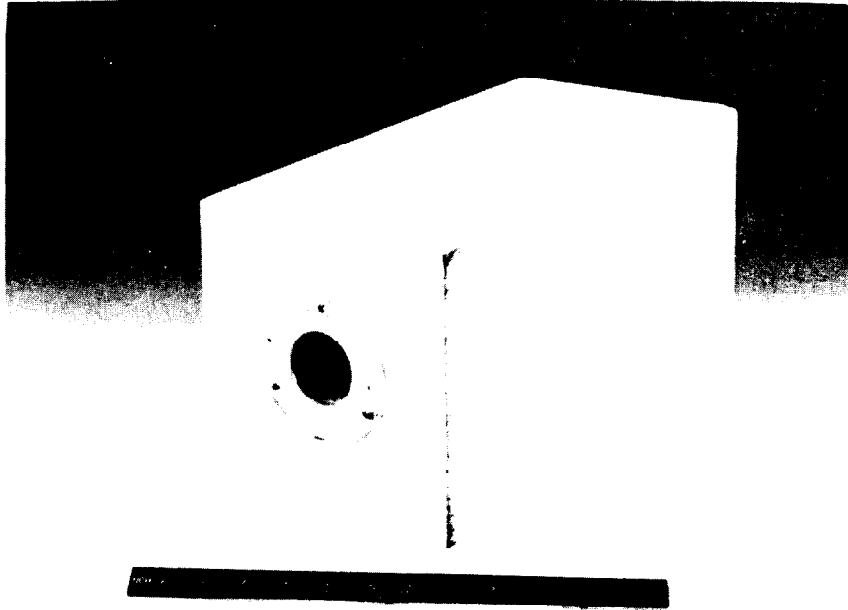


Figure 5. Boxed HEPA filter that was used in our simulation exposure test

The exposure test was designed to simulate conditions in the HE dissolution operation which consists of spraying heated DMSO for six hours to dissolve the HE. The inlet valve to the workstation is closed during the spraying operation to contain the DMSO/HE solution. The Fischer valve maintains a -1 inch pressure within the workstation during the dissolution by intermittently opening for short periods when the box vacuum drops below -1 inch due to thermal expansion of the air, leaks in the workstation, and evaporation of the solvent. We estimate that an exhaust flow of about 1 cfm is pulled through the HEPA filter during the six hour dissolution process. After the dissolution is complete, the DMSO spray is turned off and the inlet valve to the workstation is opened and the workstation is swept clean with room air for about 30 minutes.

We set up two different flow systems to simulate the HE dissolution operation. Figure 6 shows the experimental apparatus used to simulate conditions during the dissolution spraying operation. An air stream containing DMSO aerosols is heated and then passed through the HEPA

filter. Heating tape wrapped around the inlet tube can raise the temperature from room temperature up to 150 F at the inlet to the HEPA filter. Two different size Laskin nozzle generators were used to generate the DMSO aerosols: a single nozzle generator and a six nozzle generator. The air flow through the small and large generators was 1.5 and 6.5 cfm respectively. All of the air passing through the filter came from the aerosol generator. The concentration of DMSO aerosols for the small and large generators was computed from filter mass measurements to be 0.083 g/cu. ft. and 0.022 g/cu. ft. respectively.

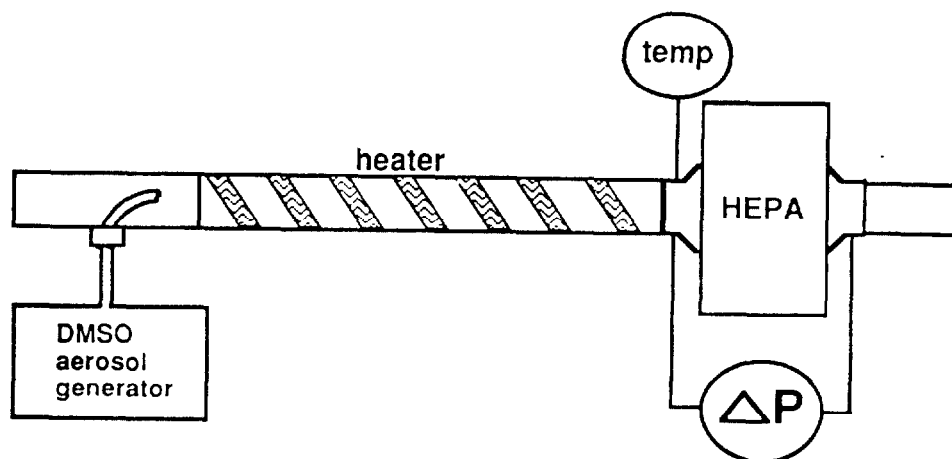


Figure 6. Schematic of apparatus used for simulating HEPA exposure to DMSO during the HE dissolution mode.

Following the 6 hour exposure to DMSO in the test apparatus shown in Figure 6, the HEPA was connected to a blower and had 30 cfm of air pass through the filter for 30 minutes. This operation represents the purge mode of the filter exposure.

The filter efficiency was also determined at the beginning of the HEPA exposure and at the end of each week of exposure for the six week test. We used a laser particle counter (Particle Measuring Systems HS-LPS) to measure the penetration of DOS aerosols throughout the HEPA filter at 50 cfm as a function of particle size from 0.065 to 1.0  $\mu\text{m}$  diameter. The DOS aerosols were generated with a Laskin nozzle generator. The upstream concentration measurement was diluted to prevent coincidence counting. A schematic of the filter efficiency test apparatus is shown in Figure 7

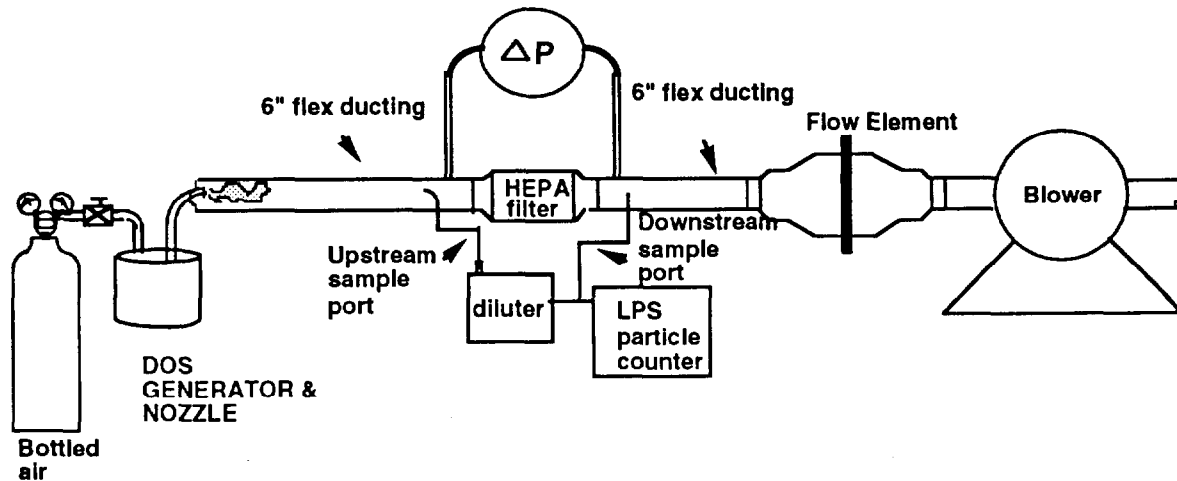


Figure 7. Schematic of filter efficiency test apparatus

For the first 81 hours of the 198 hour test, the HEPA filter was exposed daily to  $2.9 \text{ g/m}^3$  of DMSO at 1.5 cfm for 6 hours followed by an air purge at 30 cfm for 0.5 hours. For the next 85 hours the HEPA filter was exposed to  $0.78 \text{ g/m}^3$  of DMSO at 6.5 cfm for 6 hours, but with no air purges. The HEPA filter had no DMSO challenge or air flow during evenings and on weekends. This allowed liquid DMSO trapped on the filter to drain from the media and/or evaporate. During the final 32 hours, the HEPA filter was exposed to a  $0.78 \text{ g/m}^3$  of aerosol generated from a solution of plastic EPON dissolved in DMSO to simulate the HE dissolved in DMSO. At the end of the test program, the filter was subjected to 100 cfm air flow ( twice its rated flow ) to see if the filter would develop structural damage.

### V. Simulation Test Results

A summary of all of the filter exposure tests are given in Table 4., where the exposure time, initial and final pressure drop, flow rate, and computed mass of DMSO deposit is tabulated. The filter was exposed to DMSO aerosols for 198 hours over a six week period. Note that although the pressure drop of the HEPA filter increased during loading, it generally

Table 4. Summary of HEPA filter exposure tests

Date	Exposure time (hrs.)	ΔP Initial (w.g.)	ΔP final (w.g.)	Test	Flowrate (CFM)	Mass of DMSO (gms)	
8/20/93	5.50	0.020	0.041	Loading (1)	1.52	41.349	
8/25/93	8.00	0.035	0.046	Loading	1.50	60.144	
	0.50	0.580	0.680	Purge	30.00	0.000	
8/26/93	8.00	0.250	0.055	Loading	1.50	60.144	
	0.50	0.700	0.650	Purge	30.00	0.000	
8/30/93	8.00	0.025	0.050	Loading	1.50	60.144	
	0.50	0.061	0.061	Purge	30.00	0.000	
8/31/93	9.50	0.025	0.046	Loading	1.50	71.421	
	0.50	0.640	0.680	Purge	30.00	0.000	
9/1/93	9.00	0.020	0.052	Loading	1.50	67.662	
	0.50	0.660	0.710	Purge	30.00	0.000	
9/2/93	8.00	0.031	0.057	Loading	1.50	60.144	
	0.50	0.660	0.680	Purge	30.00	0.000	
9/3/93	8.00	0.025	0.047	Loading	1.50	60.144	
	0.50	0.640	0.670	Purge	30.00	0.000	
9/7/93	8.50	0.024	0.054	Loading	1.50	63.903	
	0.50	0.670	0.690	Purge	30.00	0.000	
9/8/93	8.00	0.030	0.061	Loading	1.50	60.144	
9/9/93	4.50	0.031	0.038	Loading	1.50	33.831	
	4.00	0.165	0.165	Loading (2)	6.50	0.000	
9/13/93	10.00	0.110	0.192	Loading	6.50	85.700	
9/14/93	10.00	0.120	0.179	Loading	6.50	85.700	
9/15/93	10.00	0.125	0.195	Loading	6.50	85.700	
9/16/93	6.00	0.170	0.190	Loading	6.50	51.420	
9/17/93	8.00	0.134	0.180	Loading	6.50	68.560	
9/20/93	10.00	0.130	0.195	Loading	6.50	85.700	
9/21/93	9.50	0.123	0.190	Loading	6.50	81.415	
9/22/93	8.00	0.135	0.190	Loading	6.50	68.560	
9/23/93	4.00	0.320	0.350	Loading	6.50	34.280	
	1.50	2.300	2.600	Loading (3)	42.00	12.855	
9/24/93	7.00	0.250	0.390	Loading (4)	6.50	59.990	
	2.00	0.390	0.430	Loading (5)	6.50	17.140	
9/27/93	8.00	0.320	0.480	Loading	6.50	68.560	
9/28/93	9.00	0.400	0.670	Loading	6.50	77.130	
9/29/93	5.50	0.600	0.980	Loading	6.50	47.135	
		5.000		Purge (6)	100.00	0.000	
<b>Notes:</b>	<b>Total DMSO Collected</b>						
	(1) DMSO is generated at 7.518 gms/hr.					on filter (gms)=	1568.88
	(2) DMSO is generated at 8.570 gms/hr.						
	(3) DMSO is generated at 8.570 gms/hr. and is put into a 42 CFM airstream						
	(4) DMSO is generated at 8.570 gms/hr.						
	(5) 8.570 gms/hr. of DMSO is collected on filter. 72.0 gms of EPON 1002F and 92.0 gms of EPON 1004F was added to 2.20 liters of DMSO						
	(6) Purge test with 100 CFM. Approximately 2.0 pints of DMSO spewed out of the downstream side of the filter and blower.						

returned to its original value at the beginning of the next test on the following day. Figure 8 shows the typical increase in filter pressure drop at 1.5 cfm during the 6 hour DMSO exposure. The elevated pressure drop had decreased to its initial value by the start of the next day's test. This increase in filter pressure drop and the subsequent decrease on sitting overnight was typical throughout the test program, even for the DMSO loadings that were not followed by an air purge.

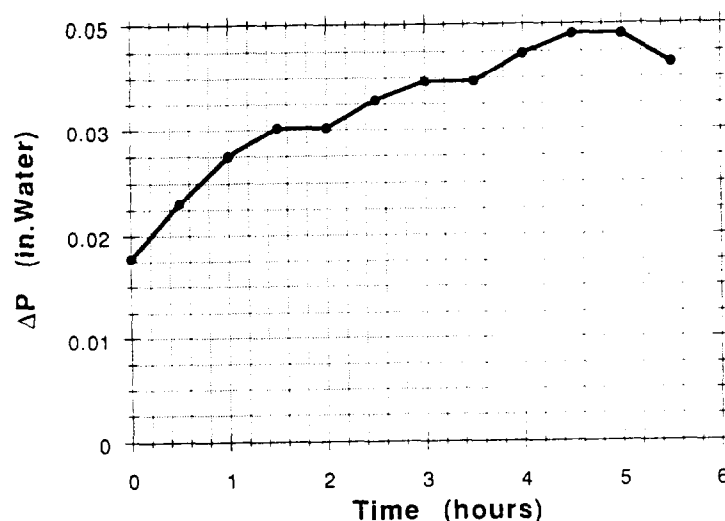
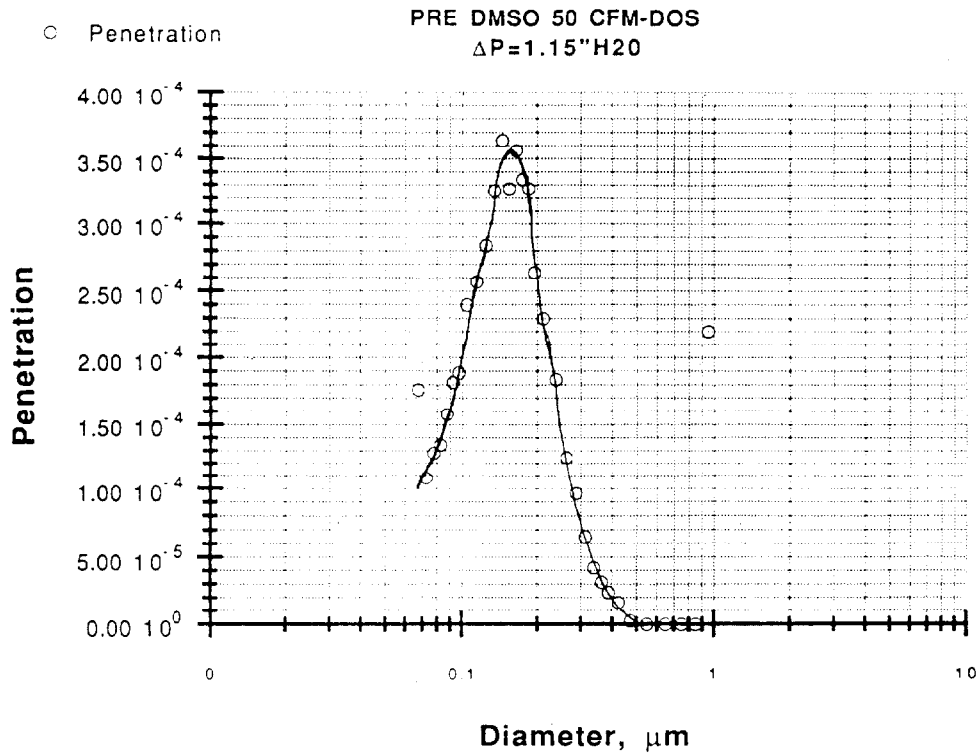


Figure 8 Typical increase in filter pressure drop during DMSO loading during the simulated HE dissolution process.

Filter penetration measurements with DOS aerosols were also conducted prior to DMSO exposure and after each week of DMSO exposures. All of the tests were conducted at the rated flow of 50 cfm. Figure 9 shows the filter penetration prior to DMSO exposure.

The filter penetration measurement after approximately every forty hours of DMSO exposure up to 166 hours was similar to the data for the fresh, unexposed HEPA filter. Although the filter pressure drop had increased from 1.15 inches to 1.55 inches after 166 hours, this increase is due to the atmospheric dust that deposited on the filter. Figure 10 shows that the filter penetration after 166 hours of DMSO exposure is comparable to the penetration for the new filter in Figure 9. It is clear from the data that exposure to DMSO will not cause a rapid degradation in HEPA filter performance.



Since the DMSO will have up to 25% dissolved HE, we conducted exposure tests on the HEPA filter with 6.3% dissolved plastic to see the effect of dissolved solids. After 32 hours of loading with the DMSO/plastic solution, the HEPA filter pressure drop increased from 0.32 inches to 0.98 inches (See Table 4) at a flow rate of 6.5 cfm. We then tried to pass 100 cfm through the loaded filter to see if the filter would be structurally damaged.

However, we quickly found that liquid DMSO was spraying out from the downstream side of the HEPA filter. By a combination of high air flow (100 cfm) and pouring out standing DMSO, we were able to remove about 1 liter of DMSO that was trapped inside the filter. According to Table 4, the computed mass of DMSO injected into the filter is 1.59 kg or 1.4 liters of liquid. Since we recovered 1 liter out of 1.4 liters, most of the DMSO aerosol injected into the filter will remain in the filter as a liquid. The HEPA filter apparently acts as a sponge soaking up liquid DMSO until the filter becomes fully saturated

After we removed the liquid DMSO from the filter, we conducted a DOS penetration test at 50 cfm and found the pressure drop had increased to 2.85 inches, and the aerosol penetration increased to 1.4%. The penetration measurements are shown in Figure 11. The significantly increased width of the penetration curve as well as the higher penetration values in Figure 11 compared to that in Figures 9 and 10 is characteristic of a filter leak. It is unlikely that a filter leak was caused by the high air flow since the total pressure drop across the HEPA was only 5 inches, and that pressure was divided between the prefilter and the HEPA filter.

We then tried to remove any residual DMSO remaining in the filter by passing heated air at 150 F through the filter. After four hours, the filter pressure drop decreased from 2.85 to 2.1 inches, and the filter penetration decreased from 1.4% to 1.1%. Three additional days of passing 50 cfm of 150 F heated air through the filter reduced the pressure drop to 1.68 inches and the penetration to 0.4%. The DOS penetration curve for the HEPA filter after the three day purge is shown in Figure 12.

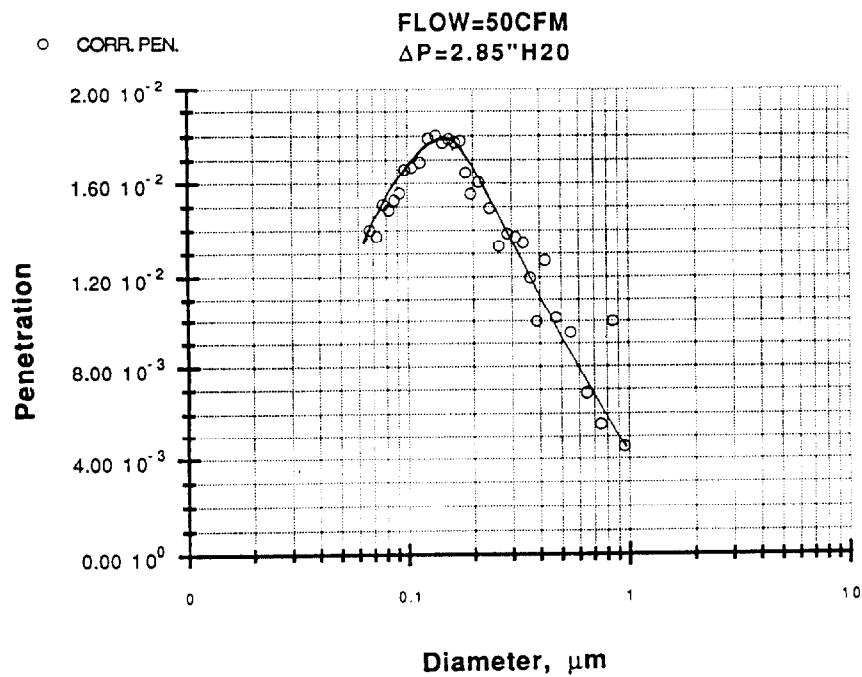


Figure 11. Penetration of DOS aerosols through HEPA filter exposed to 198 hours of DMSO aerosols followed by 32 hours of DMSO/dissolved plastic aerosols.

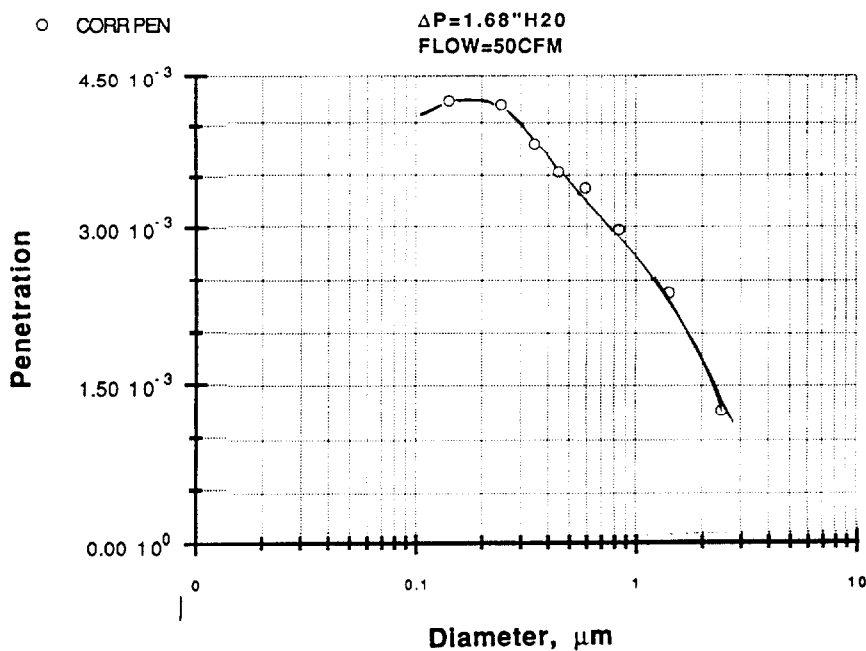


Figure 12. Penetration of DOS aerosols through HEPA filter after three days of purging with 50 cfm of heated air

## 23rd DOE/NRC NUCLEAR AIR CLEANING AND TREATMENT CONFERENCE

A summary of all the penetration measurements made in this evaluation is given in Table 5.

Table 5. Summary of penetration and pressure drop tests.

Exposure (Hours)	Pressure Drop (Inches Water)	Penetration at 0.3 $\mu\text{m}$
0	1.15	$8 \times 10^{-5}$
6	1.25	$8 \times 10^{-5}$
56	1.32	$6 \times 10^{-5}$
81	1.25	$9 \times 10^{-5}$
120	---	---
166	1.55	$1.1 \times 10^{-4}$
198	2.85	$1.4 \times 10^{-2}$
+	2.10	$1.1 \times 10^{-2}$
++	1.68	$4.0 \times 10^{-3}$
+++	1.30	$3.0 \times 10^{-4}$
+	After purging with 50 cfm air at 150°F for 4 hours	
++	After purging with 50 cfm air at 150°F for 3 days	
+++	HEPA requirements	

We can attribute the changes in filter performance to the residual DMSO in the filter that was driven off by heated air. The filter pressure drop and the penetration decreased from 2.85 inches to 1.68 inches and from 1.4% to 0.4% respectively by passing heated air through the filter. The remaining effects are due to the atmospheric dust deposits and the permanent structural damage from the DMSO attack on the HEPA filter. Table 5 shows that the pressure drop increased by about 0.1 inch of water for each 40 hour week of operation except for the final week when liquid DMSO had saturated the filter. However, once the DMSO was driven off by heat, the increase in pressure drop for the final week was also about 0.1 inch. This pressure drop increase is most likely due to the atmospheric dust that has accumulated on the filter. The accumulation of atmospheric dust is seen as the darkened center of the filter pack in Figure 13. The front end of the wooden box was cut open to expose the filter.



Figure 13. Inlet side of the prefilter-HEPA filter with end cut open to expose the media. Note the dust accumulation in the center of the media pack.

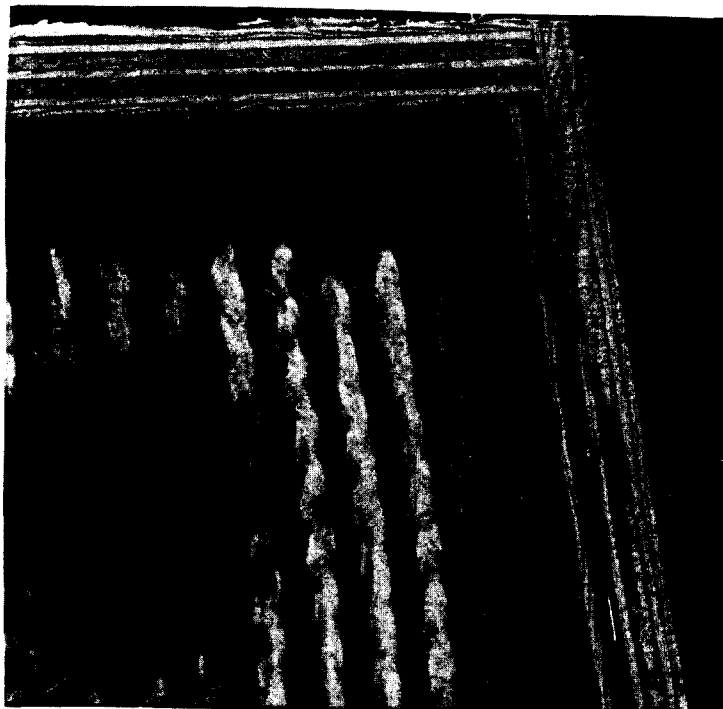


Figure 14. Close-up of upper right corner of Figure 13 showing a crack in the urathane sealant between the wooden frame and the media pack. This crack is a leak path.

We cut the HEPA filter open to expose the inlet and exit filter faces to determine if we could see signs of physical degradation that could explain the increased filter penetration. Figure 14 shows that there is a small crack in the sealant between the wooden frame and the filter pack. This crack was found to be one of two leaks that produced the higher aerosol penetration

We also found that the DMSO exposure created cracks and warped the plywood frame of the HEPA. Figure 15 shows the exterior corner of the plywood frame with the paint blistering and the edges separating due to warpage. Figure 16 is a cut-away portion of the same corner and shows a direct leak path from the interior to the exterior of the HEPA box. Since the leak path is on the inlet side of the HEPA, it can not be the cause of the increased aerosol penetration because any particles leaking into the box would be filtered.

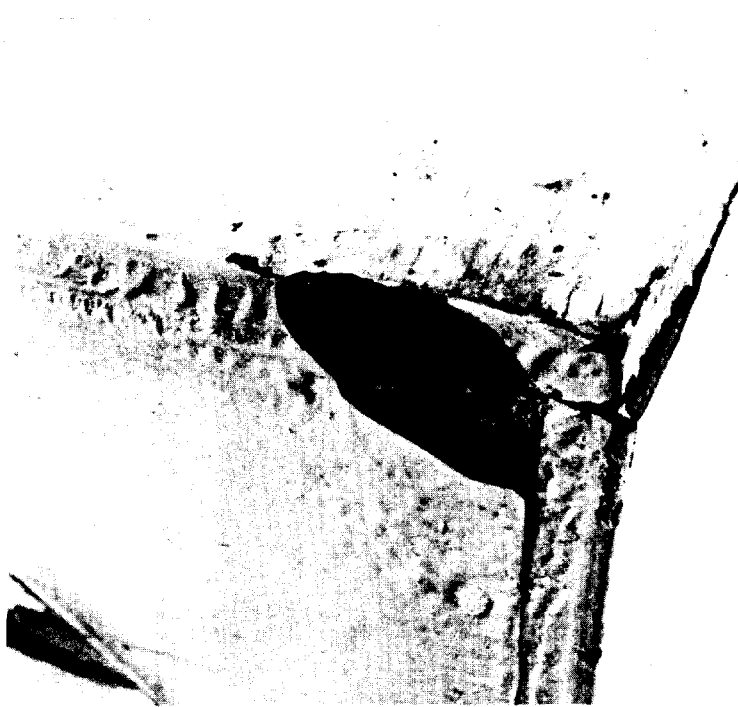


Figure 15. Photograph of a corner of the HEPA filter showing box warpage and joint separation.

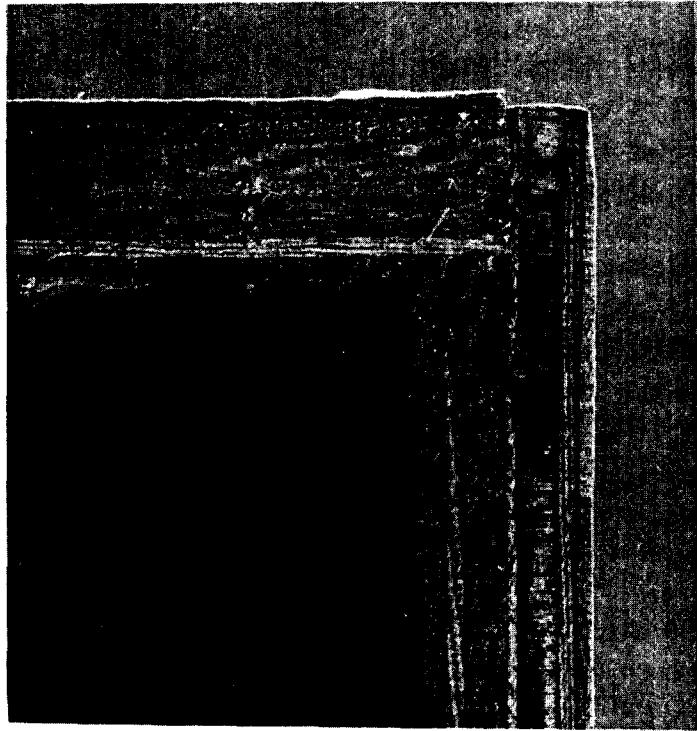


Figure 16. Photograph of cut-away portion of the corner in Figure 15. Note the direct leak path at the corner.

We conducted a series of scan tests to verify that the cause of the filter failure was due to the crack in the sealant between the filter pack and the plywood frame shown in the upper right corner of Figure 14. The scan test consisted of scanning across the open filter face (inlet side with prefilter) with a 1/4 inch probe and measuring the DOS concentration with a light scattering photometer (Phonex Precision Instruments, model JM-7000). DOS aerosols were injected in the opposite filter face with a 5 cfm air stream. Measurements confirmed that aerosols were leaking through the visible crack in the upper right corner. A similar leak was also detected on the bottom right corner, although no visible crack was seen. The filter was then reversed and another scan made across the filter face (exit side with HEPA filter). The scan measurements showed leaks on the upper and lower left corners between the sealant and the plywood frame, and directly opposite from the leaks on the other side. There were no visible cracks. It appears that the leak path between the sealant and frame runs along the entire filter depth.

## VI. Preliminary Field Test Results

We evaluated the HEPA filter that was used in trial tests for removing HE from mock warheads to see if there was any deterioration in performance. The filter was a dual-stage prefilter-HEPA filter unit manufactured by Donaldson and similar to the boxed unit in Figure 5, but with a 135 cfm capacity. The larger capacity HEPA filter was used to reduce the restriction in the exhaust flow compared to the standard 50 cfm filter used in our laboratory tests. The filter had been exposed to a total of 50 hours of DMSO/HE exposure: 5 hours of the venting phase when the exhaust valve was open and 45 hours of the dissolution phase in which hot DMSO is sprayed against the HE. We estimate the exhaust flow was about 5 cfm during this dissolution process. Unfortunately, the work station was not instrumented to provide a measure of the exhaust flow or the pressure drop across the HEPA filter.

The test apparatus for measuring the filter penetration and the pressure drop is shown in Figure 8. Prior to conducting the penetration tests, we monitored the downstream flow for potential HE release, but found none. The results of the penetration measurements at 135 cfm and 27 cfm are shown in Figures 17 and 18 respectively. The filter penetration values at 0.3  $\mu\text{m}$  are .006% and .0004% at 135 cfm and 27 cfm respectively. The corresponding pressure drop measurements are 1.80 inches and 0.30 inches at 135 cfm and 27 cfm respectively. For comparison the filter certification tests on the new filter at the Rocky Flats Filter Test Station showed the penetration was less than .01% for both 135 cfm and 27 cfm. The only pressure drop recorded was 2.2 inches at 135 cfm. We suspect that restriction in the adapters used to connect to the boxed HEPA filter was responsible for the higher initial pressure drop.

The preliminary data suggests that there was no degradation in filter efficiency or pressure drop within the 50 hours of DMSO/HE exposure. If the HEPA degradation for the 135 cfm HEPA follows the same trend as seen for the 50 cfm HEPA filter, then no degradation would be seen until about 200 hours of DMSO exposure. The field evaluation was clearly too short to see any loss in HEPA performance.

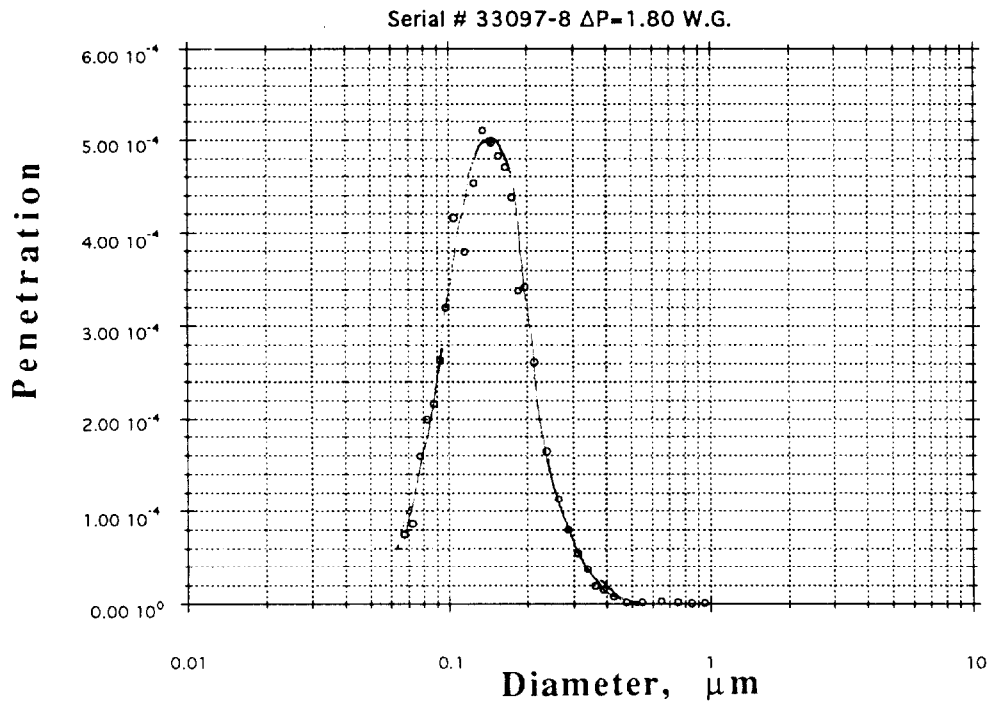


Figure 17. Penetration of DOS aerosols through 135 cfm HEPA filter at 135 cfm after 50 hours exposure to DMSO/HE

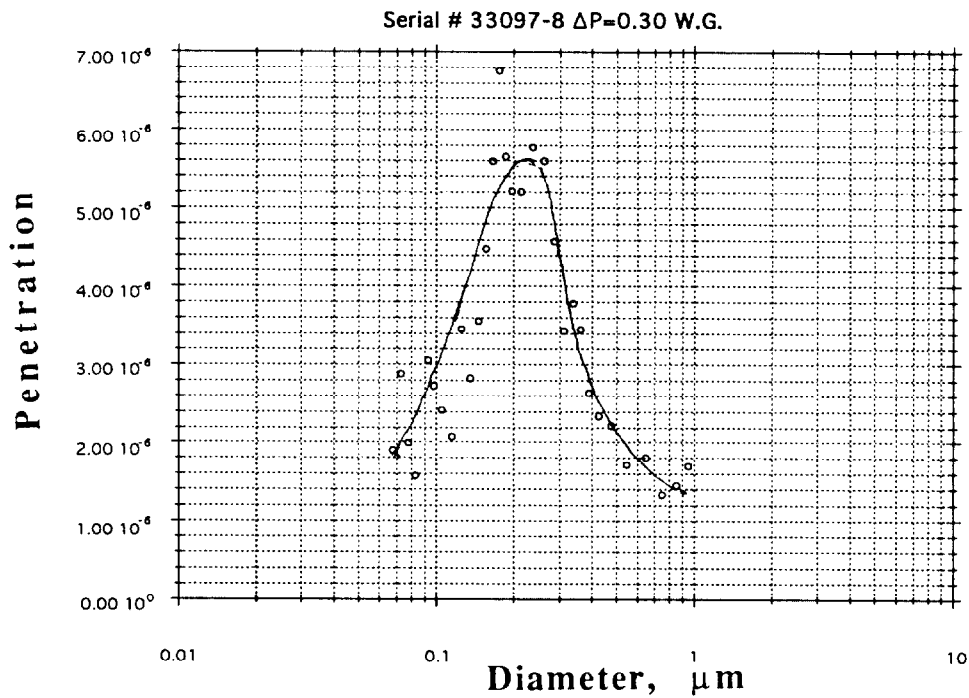


Figure 18. Penetration of DOS aerosols through 135 cfm HEPA filter at 27 cfm after 50 hours exposure to DMSO/HE

## V. Conclusions

Preliminary tests show that DMSO aerosols degrade the performance of HEPA filters over time by chemical attack to create leak paths and by saturating the filter media to increase both the pressure drop and the aerosol penetration. A 50 cfm HEPA filter was exposed to DMSO aerosols for 198 hours under conditions that simulate the HE dissolution operations in weapons dismantlement. The efficiency for 0.3  $\mu\text{m}$  particles decreased from 99.992% to 98.6%, and the pressure drop increased from 1.15 inches to 2.85 inches during the exposure. We found that most of the DMSO aerosol that was captured by the HEPA filter had condensed in the filter as a pool of liquid. Since the efficiency of the HEPA filter drops below the minimum allowed efficiency of 99.97%, it has to be replaced with a new filter.

The larger portion of the decreased efficiency and increased pressure drop is due to the DMSO saturation of the HEPA filter media. Of the 1.39% decrease in efficiency, 1.00% is due to the saturation, while 0.39% is due to the leak paths. Of the 1.70 inches increase in pressure drop, 1.17 inches is due to the saturation, while 0.53 inches is due to the atmospheric dust that was not prefiltered in our experiments. We were able to isolate the effect of the DMSO saturation by driving off the liquid with heated air. The difference in efficiency and pressure drop before and after the DMSO is driven off can be attributed to the DMSO saturation. Loss in filter performance due to liquid saturation or partial saturation is not unique to DMSO, but applies to all liquids.

The smaller portion of the decreased efficiency in these preliminary tests is due to the leak paths generated by DMSO attack. The DMSO had produced two leak paths between the polyurethane sealant and the plywood frame. One of the leak paths was visible in the photograph in Figure 14 where the sealant was separated from the plywood frame. Although the penetration due to the leak path is about one third of the total penetration, the 0.39% penetration due to the leaks is still more than ten times the allowed 0.03% penetration. The filter would have to be replaced.

The DMSO exposure also produced visible cracks and warpage on the inlet portion of the plywood frame as shown in Figures 15 and 16. Although the cracks formed a leak path to the exterior of the filter, the leak was not measured as an increase in aerosol penetration because the filter was under vacuum, and the ambient aerosols would be filtered. We

believe that the accumulated DMSO liquid in the boxed HEPA filter is responsible for both the plywood warpage and the creation of leak paths due to separation of the sealant from the plywood frame.

The efficiency of the two exhaust HEPA filters in Figure 1 to remove potential radioactive or DMSO/HE aerosols depends on the exhaust flow rate, the particle size distributions of the aerosols, and any degradation resulting from DMSO exposure. Although most of the DMSO aerosols will be trapped in the first HEPA filter, a large fraction of DMSO vapor may pass through the first filter and condense on the second HEPA filter and cause degradation. Since the HE is not volatile, it will remain on the first filter except for the small fraction that passes through as an aerosol. Thus the combined efficiency for a degraded first filter (98.6%) and a standard second filter (99.97%) is 99.99996% for 0.3 $\mu$ m particles. If both filters are degraded (98.6% ) by DMSO attack, then the combined efficiency will be 99.98%. If the first filter is replaced prior to its degradation, each of the filters will have 99.97% efficiency, and the combined efficiency will be 99.999991%. The collection efficiency for DMSO/HE aerosols will be much higher because the particle size is much greater. However, if liquid DMSO/HE is allowed to accumulate in the filter, it can flow unobstructed through the filter, thereby leaving only the second HEPA filter for stopping the DMSO/HE aerosols. In this case the overall efficiency for the two filters is 99.97% for 0.3  $\mu$ m particles.

## VI Recommendations

We recommend that the first stage HEPA filter from the DMSO dissolution workstation be replaced after 160 hours of exposure. If the pressure drop across the HEPA filter increases by more than 50% of its initial value, then the filter should also be replaced even if the exposure is less than 160 hours. This will assure that the HEPA filter will not be degraded if different operating conditions cause accelerated filter saturation. The first stage HEPA filter should also be mounted in a vertical configuration to promote liquid drainage into the workstation. The second stage HEPA filter also should be monitored (pressure drop increase) for DMSO accumulation due to condensation from the vapor. If the pressure drop increases by 50% of its initial value, the second stage HEPA should be replaced.

We also recommend that the filters removed from the dissolution workstations be evaluated for filter efficiency and examined for any

structural damage. This will provide a data base for defining the HEPA degradation under actual field conditions.

## VII. Acknowledgement

The authors thank Mr. Derek Wapman, Project Manager of the LLNL HE Dissolution Workstation Project, for his support and for many helpful discussions and suggestions.

## DISCUSSION

**GOOSSENS:** I wonder why you do not use a high efficient mist eliminator (HEME) as we have introduced in the PAMELA off-gas treatment circuit.

**VENDEL:** Our mist eliminators remove all particles of 1.5  $\mu\text{m}$ .

**BERGMAN:** Thank you for your suggestion. We will certainly take a closer look at mist eliminators in our future work. We initially considered installing a mist eliminator but decided not to use one because of the added space requirement, the small size of DMSO droplets, and the limited ventilation system. We were worried that the existing ventilation system only had 6 inches of vacuum and could not accommodate a high efficiency mist eliminator in addition to the two HEPA filters.

**VENDEL:** It was manufactured by an American company?

**BERGMAN:** Yes.

**FIRST:** The US-approved mist eliminator that has gone into a number of nuclear power plants is tested at a droplet size of about 3  $\mu\text{m}$ . When particle size decreases, it still has significant efficiency. In other words, it does not get below 80% efficiency until you get well down into the fractional micrometers. Therefore, when you have a very deep, dense eliminator, such has been put into nuclear plants, I think it would do a good eliminator job, even on 1.5  $\mu\text{m}$ ; it would protect the HEPA filter for quite a long time. On the other hand, if you think of a prefilter as one of these half-inch thick mesh or fiber units, of course it will not be very efficient.

**BERGMAN:** We were thinking of the half-inch mesh kind that they put in front of HEPA filters. You made an excellent suggestion and I think I will amend the paper accordingly.

PROPOSED RETROFIT OF HEPA FILTER PLENUMS WITH INJECTION  
AND SAMPLING MANIFOLDS FOR IN-PLACE FILTER TESTING

Jan K. Fretthold

EG&G Rocky Flats, Inc.  
P.O. Box 464  
Golden, CO 80402

Abstract

The importance of testing HEPA filter exhaust plenums with consideration for As Low as Reasonably Achievable (ALARA) will require that new technology be applied to existing plenum designs.

I. Introduction

HEPA filter in-place testing at Rocky Flats has evolved slowly due to a number of reasons. The first plenums were built in the 1950's preceding many standards. The plenums were large which caused air dispersal problems. The systems were variable air flow. Access to the filters was difficult. The test methods became extremely conservative. Changes in methods were difficult to make. The acceptance of new test methods has been made in recent years with the change in plant mission and the emphasis on worker safety.

II. History of In-place Testing at Rocky Flats Plant

The Rocky Flats Environmental Technology Site, Department of Energy (DOE), utilizes approximately eleven thousand, size 5, HEPA filters in supply and exhaust systems. Eight thousand filters are used for PU Operations. The filter plenums that house the HEPA filters contain from three filters per stage of filtration to six hundred and twenty filters per stage. The filter plenums have from 2 stages of filtration to four stages.

Early in the history of Rocky Flats (e.g., the 1950s and 1960s), in-situ mass flow testing of filter plenums was performed. This method flooded the upstream filter plenum with DOP, and measured the concentration downstream of the HEPA filters. In the 1970s, this method was changed to one of testing individual HEPA filters because the size of the filter plenums precluded full plenum flooding with DOP. In this revised testing, personnel entered the filter plenum upstream of the HEPA filter being tested and sprayed DOP aerosol at the filter. Concurrently, personnel in the filter plenum downstream of the HEPA filter being tested scanned the filter to measure the individual filter efficiency. (See Figure 1). The average of all the filters was used for the stage efficiency.

In the 1980s, further improvements were made. A separate Filter Test Group was formed to provide single-point accountability for HEPA filter testing.

## 23rd DOE/NRC NUCLEAR AIR CLEANING AND TREATMENT CONFERENCE

These personnel received detailed training in HEPA filter testing. Management personnel attended formal off-site training. The Filter Test Group formalized procedures for in-place testing of HEPA filters. To ensure consistency of measurements, enhancements were made to existing filter test practices, including utilization of a shroud to direct DOP to the specific filter being tested. (See Figure 2).

In 1994 a test shroud, (as in Figure 3), was put into use on the downstream of the HEPA filter. The use of the shroud greatly reduced the filter test time but still required the test personnel to enter the filter plenum.

### III. Project Description

The goal of the project is to determine the type of in-place test manifold which can be best utilized in existing filter plenums at the Rocky Flats Site. We will use an existing "New" filter plenum for testing manifold systems; we will evaluate existing manifold system designs in use at other sites; and we will try to minimize the physical modifications required to install a manifold system in the existing filter plenums.

### IV. Facility

The test site selected is a building that was slated for use as a waste packaging facility, (as in Figure 4). The process requirements changed, leaving the building open for other uses.

A new addition had been added to the building just prior to shut down of the process. The new section included two filter plenums which were never put on line. (See Figure 5). The plenum selected for the testing is located on the ground floor. (See Figure 6). It is a two (2) stage walk-in unit with nine (9) filters per stage, air locks, (as in Figure 7), and a deminster section.

The modifications required to this system are minimal. The two system fans will require control modifications to enable them to be run simultaneously for CFM variations. The inlet duct system will require modification. The duct will be disconnected from the process area and routed to bring air in from outside the building.

### V. Manifolds

Three styles of injection manifolds will be installed and tested. Modifications to these will be made to optimize their design. Style One will be a duct inject type installed in the inlet duct, using the plenum inlet deflector plate and the deminster section to mix the challenge. Style Two, a pipe grid manifold (see Figures 11 and 12) and Style Three, an air injected deflector (see Figure 13) will be installed between stages of filtration, air flow will supply the mixing.

Sample manifolds will be installed upstream and downstream of the filter stages. The manifold will take a sample at each filter. (See Figure 14). Additionally a exhaust duct sample point will be evaluated.

## 23rd DOE/NRC NUCLEAR AIR CLEANING AND TREATMENT CONFERENCE

The plenum window ports will be modified for hose connections to introduce the test challenge and take samples. (See Figure 15).

Qualification of the test method will follow ASME N-509 and N-510 Standards. The test plenum is similar to on-line plenums allowing for simulation of air flows and mixing patterns.

### VI. Additional Test Plenum Uses

The filter plenum manifold development project will involve a number of side projects. The evaluation of a Los Alamos National Laboratory laser spectrometer in-place test system and it's use with the manifold system (this system allows the testing of two filter stages at the same time). (See Figure 16).

The testing of the effect of a fire water spray system on HEPA filters. (See Figure 8).

The sample line loss for various material and lengths of run.

The evaluation of a filter hold down system to replace the multiple filter hold downs now in use. (See Figure 9).

The development of a X-Y scan method for material collected on filters.

The plenum will also provide a training location. The system can be expanded to provide simulation D & D mock ups.

### VII. Program Status

The project was begun in fiscal year 1993. Equipment was purchased and Engineering was completed. The project was unfunded for fiscal year 1994. The request for funding was submitted for fiscal year 1995.

### VIII. Conclusion

This project is a research and development project with two driving forces, ALARA and Cost Savings. We are open to any suggestions.

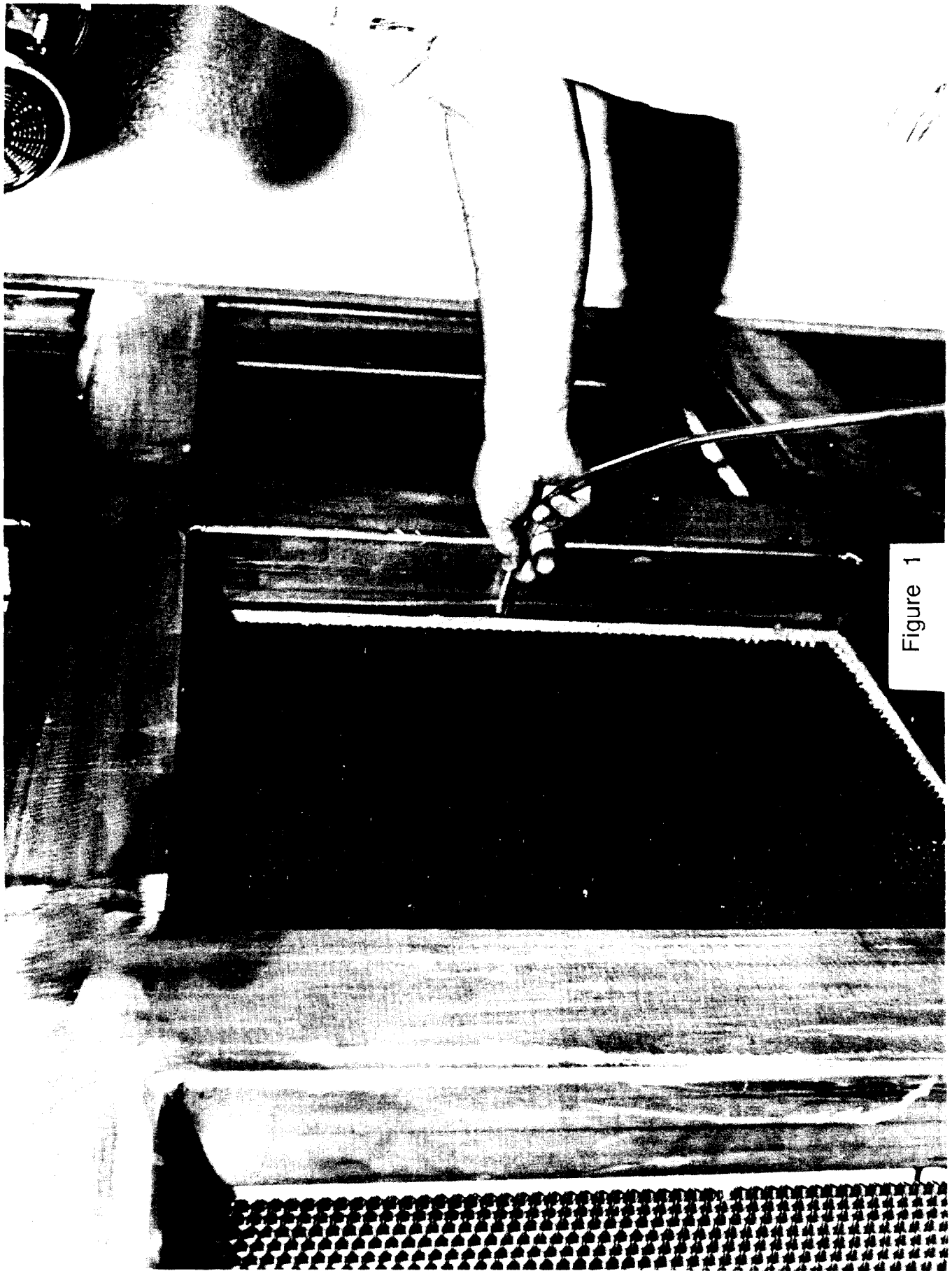


Figure 1

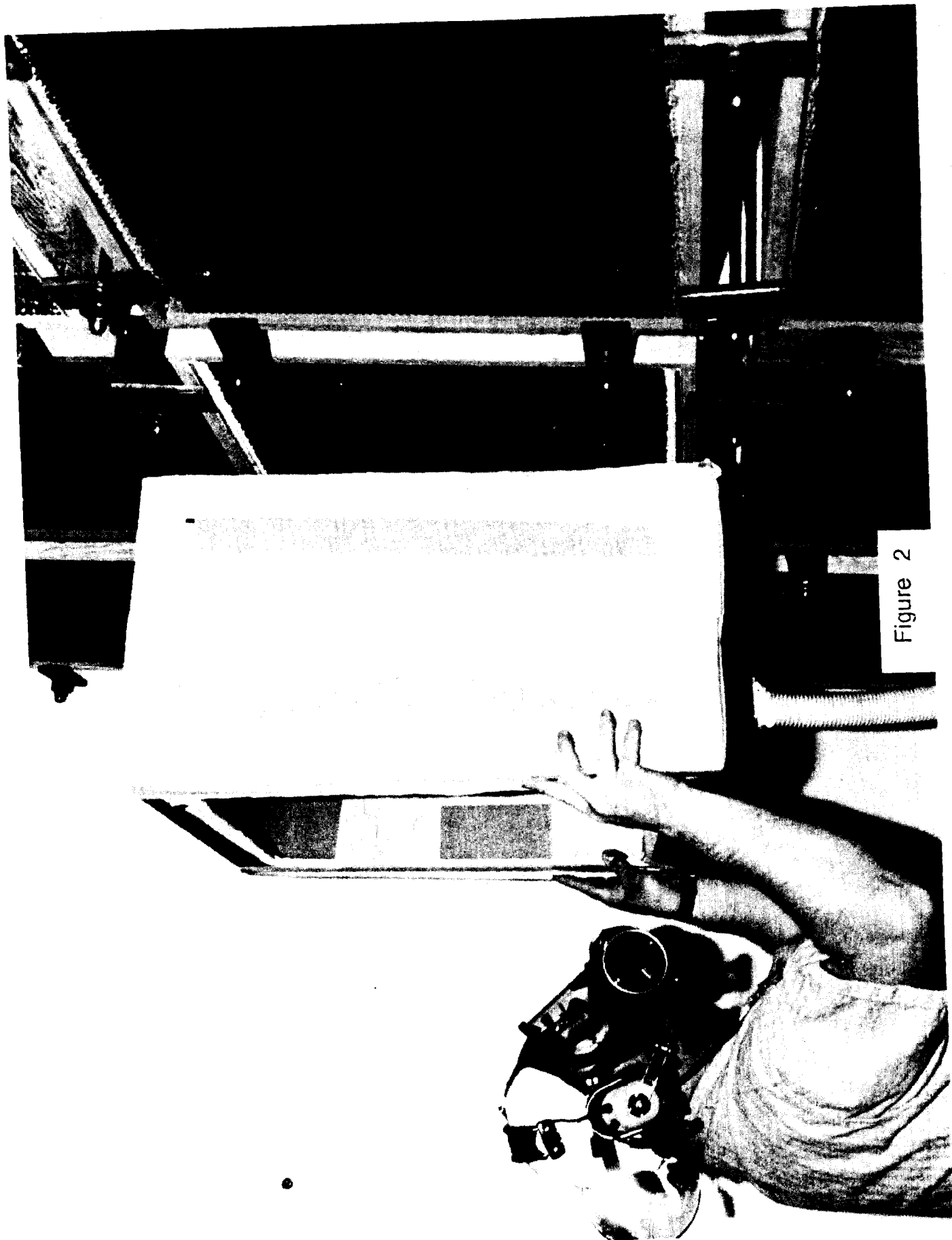


Figure 2

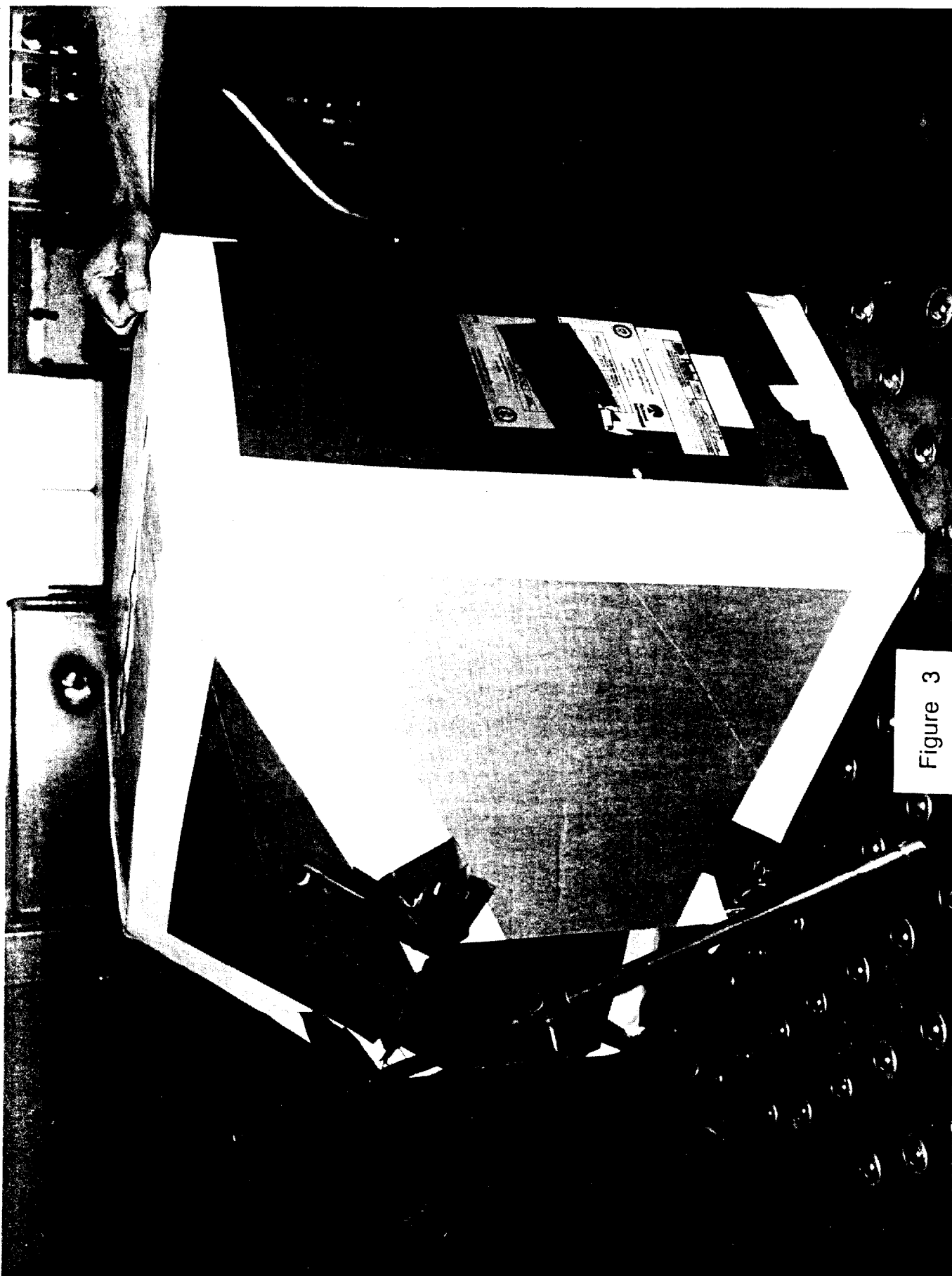


Figure 3

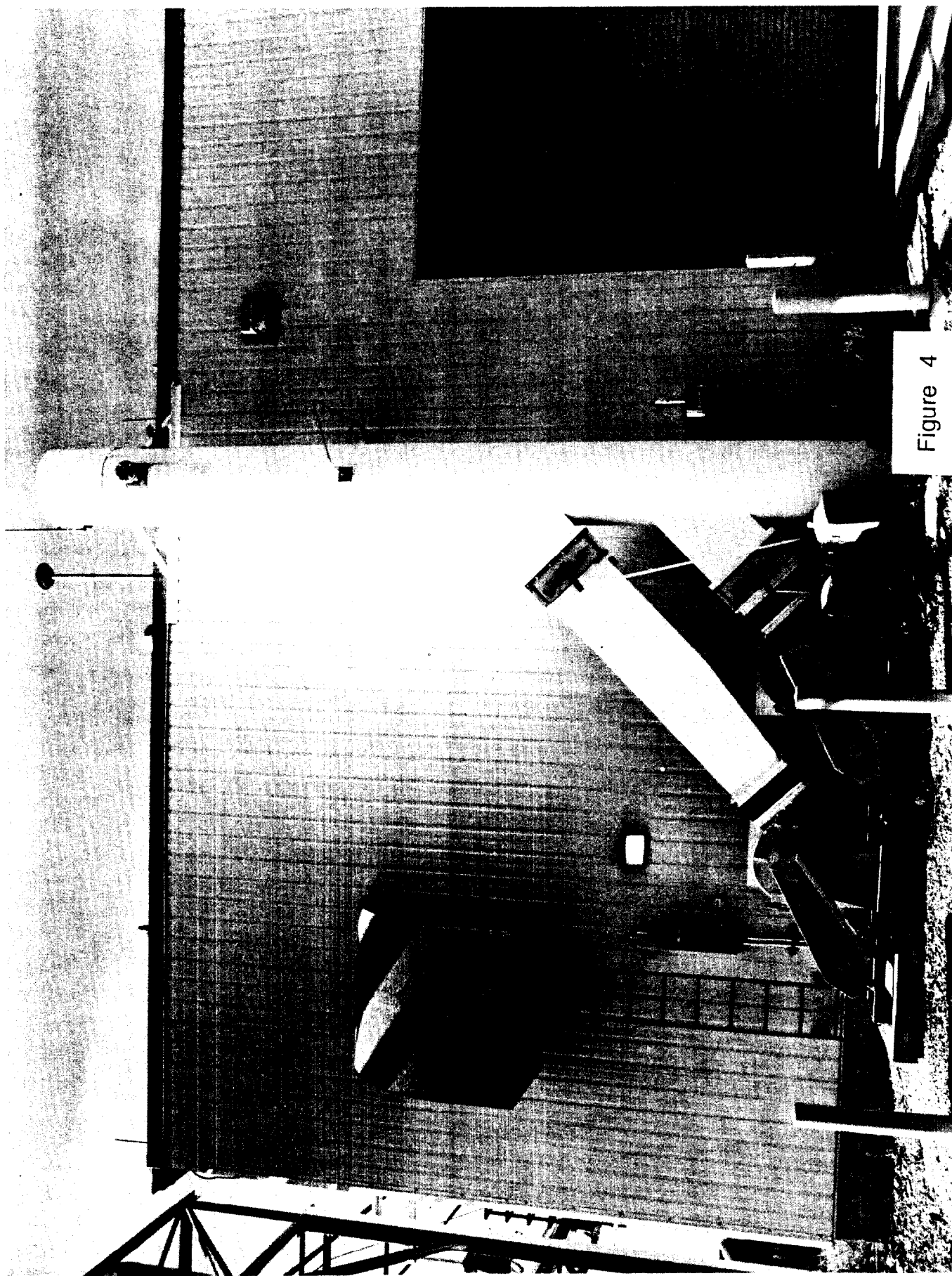


Figure 4

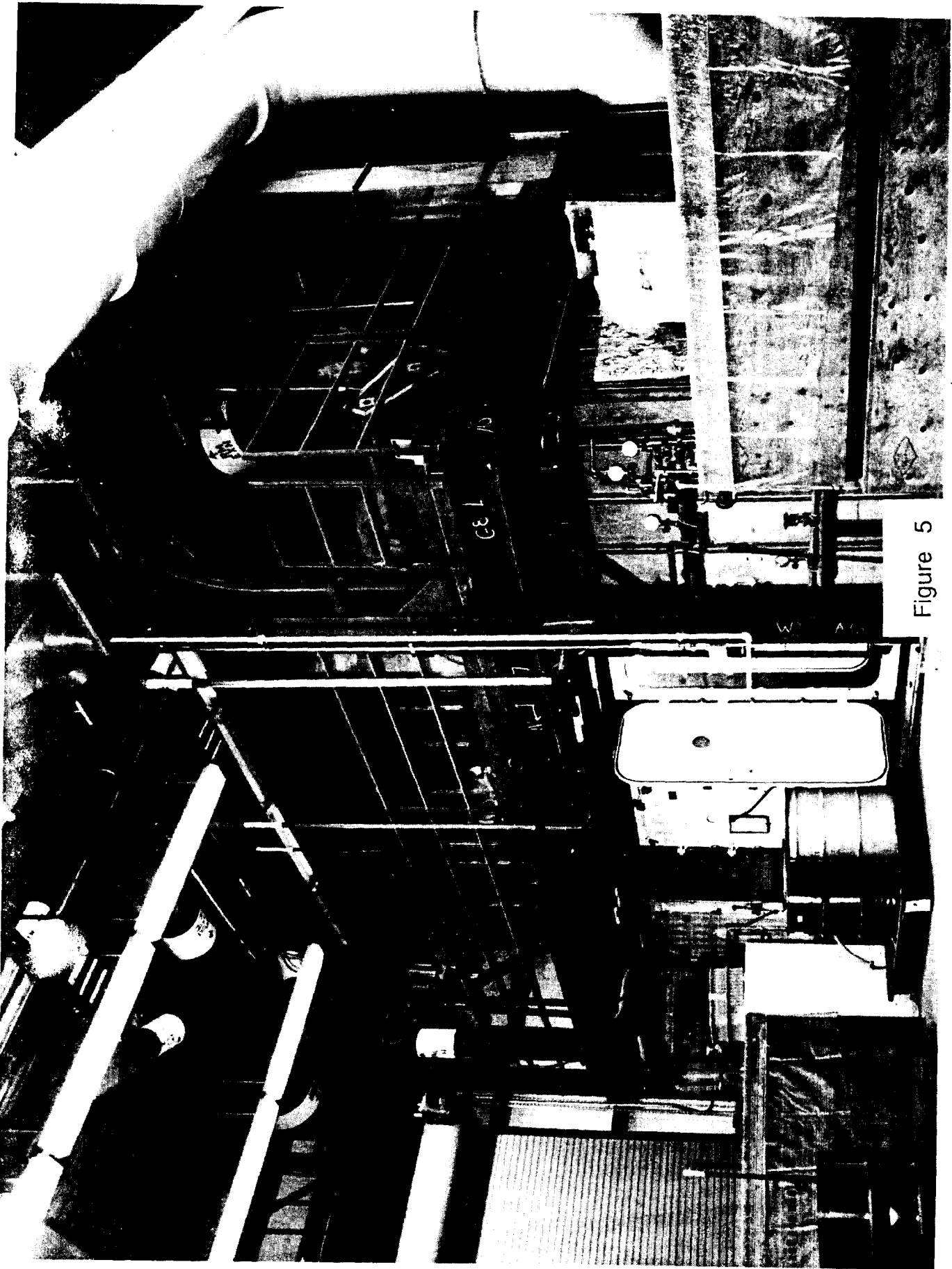


Figure 5

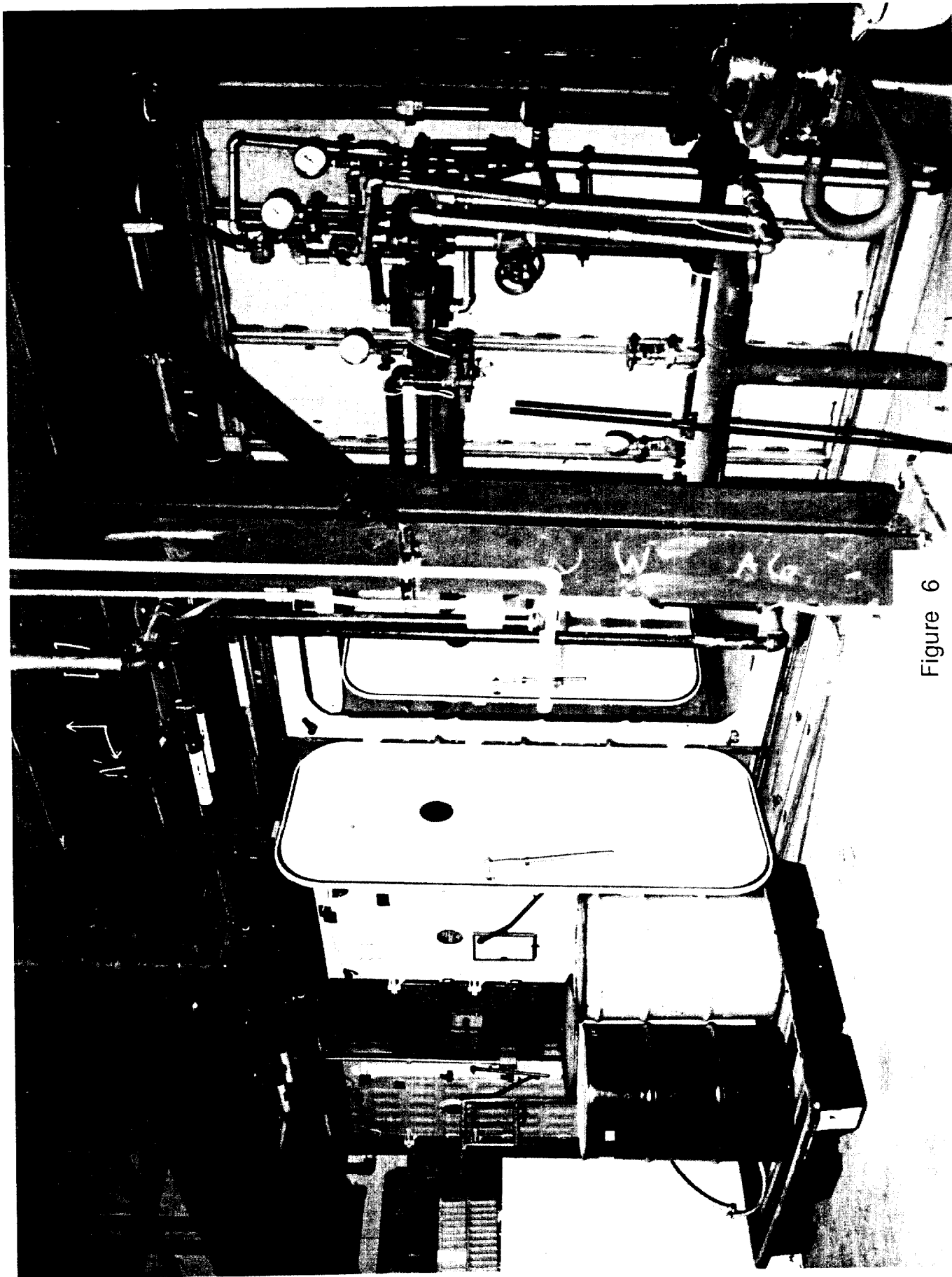


Figure 6

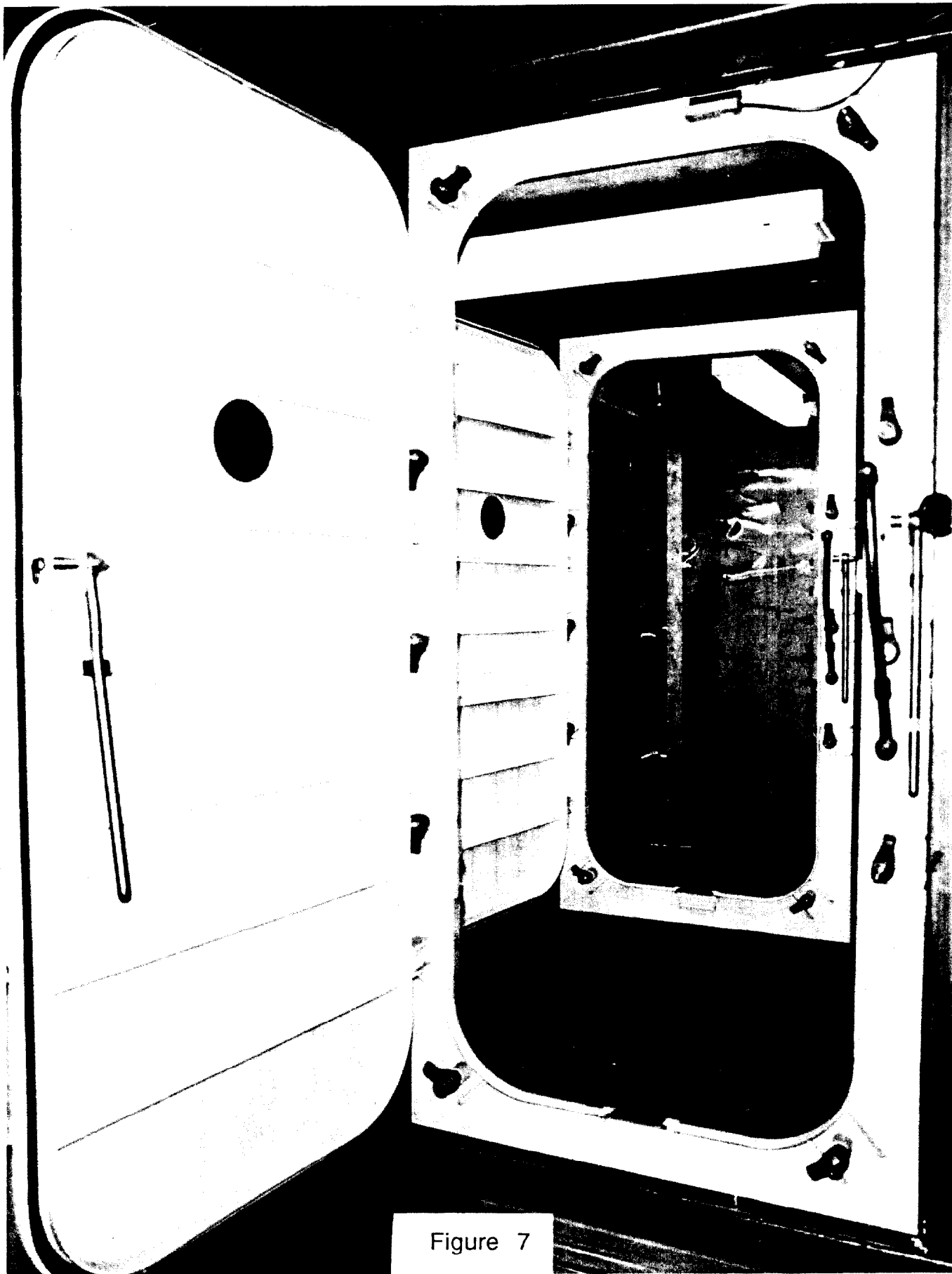


Figure 7



Figure 8

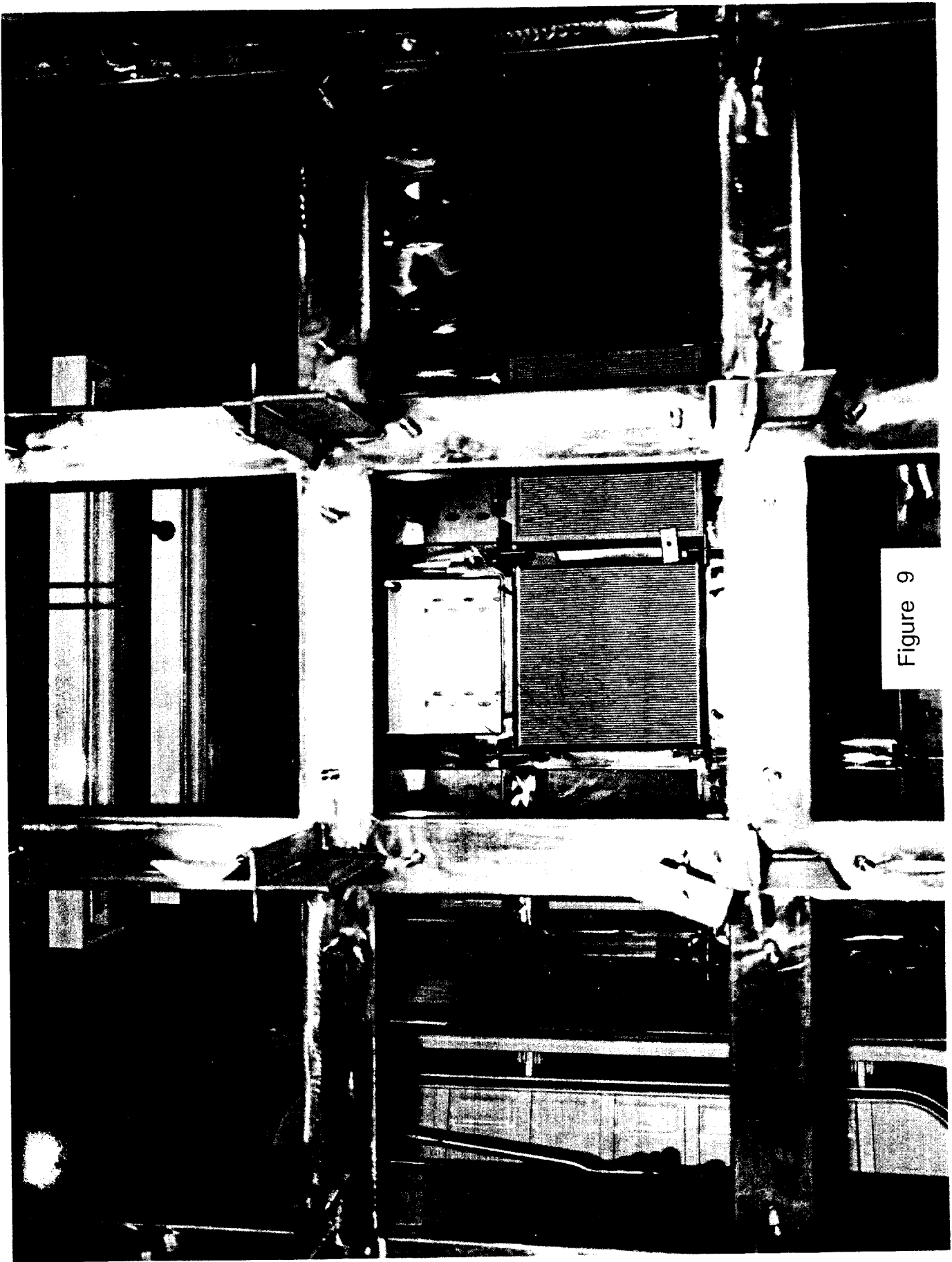


Figure 9



Figure 10

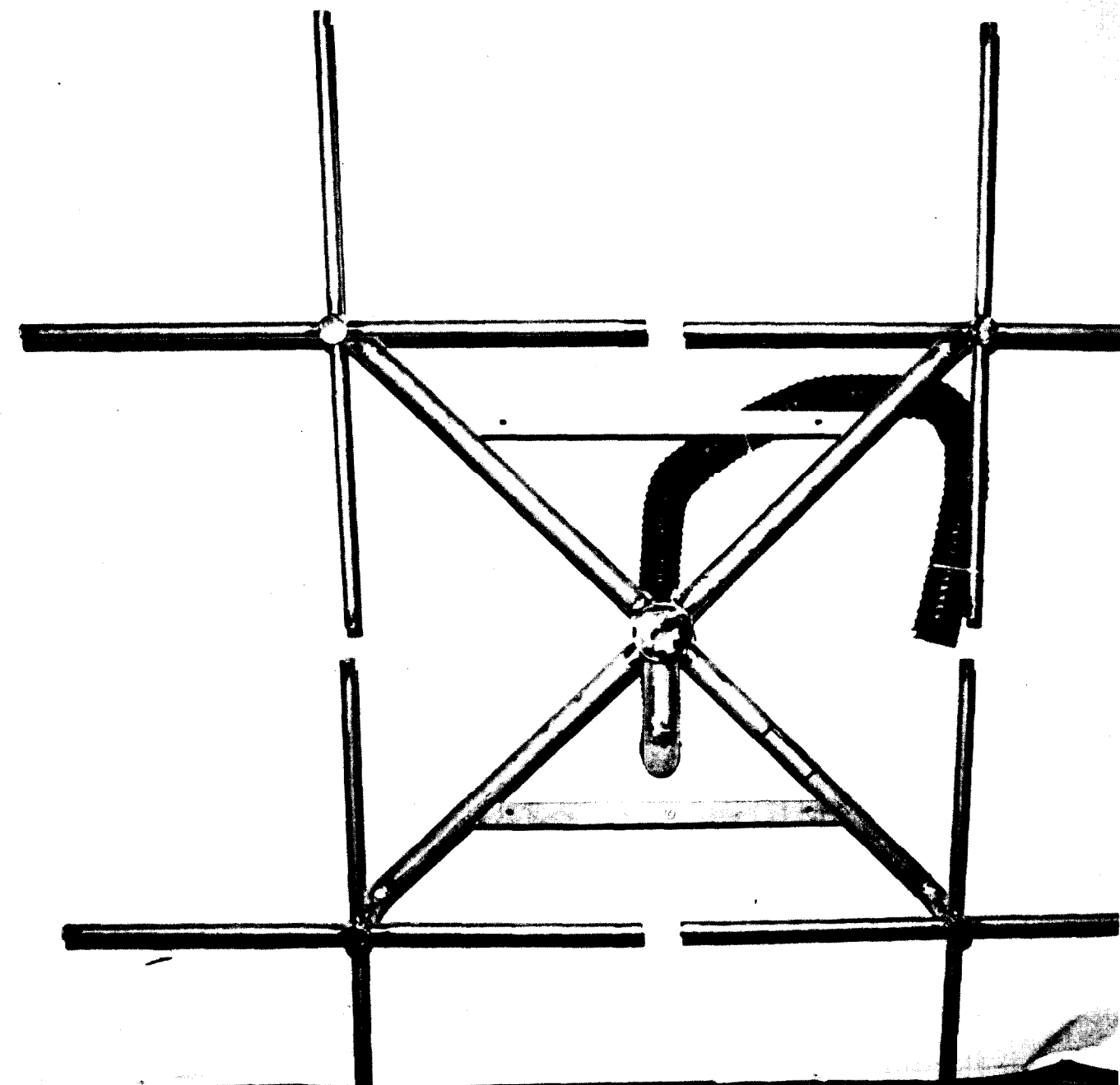


Figure 11

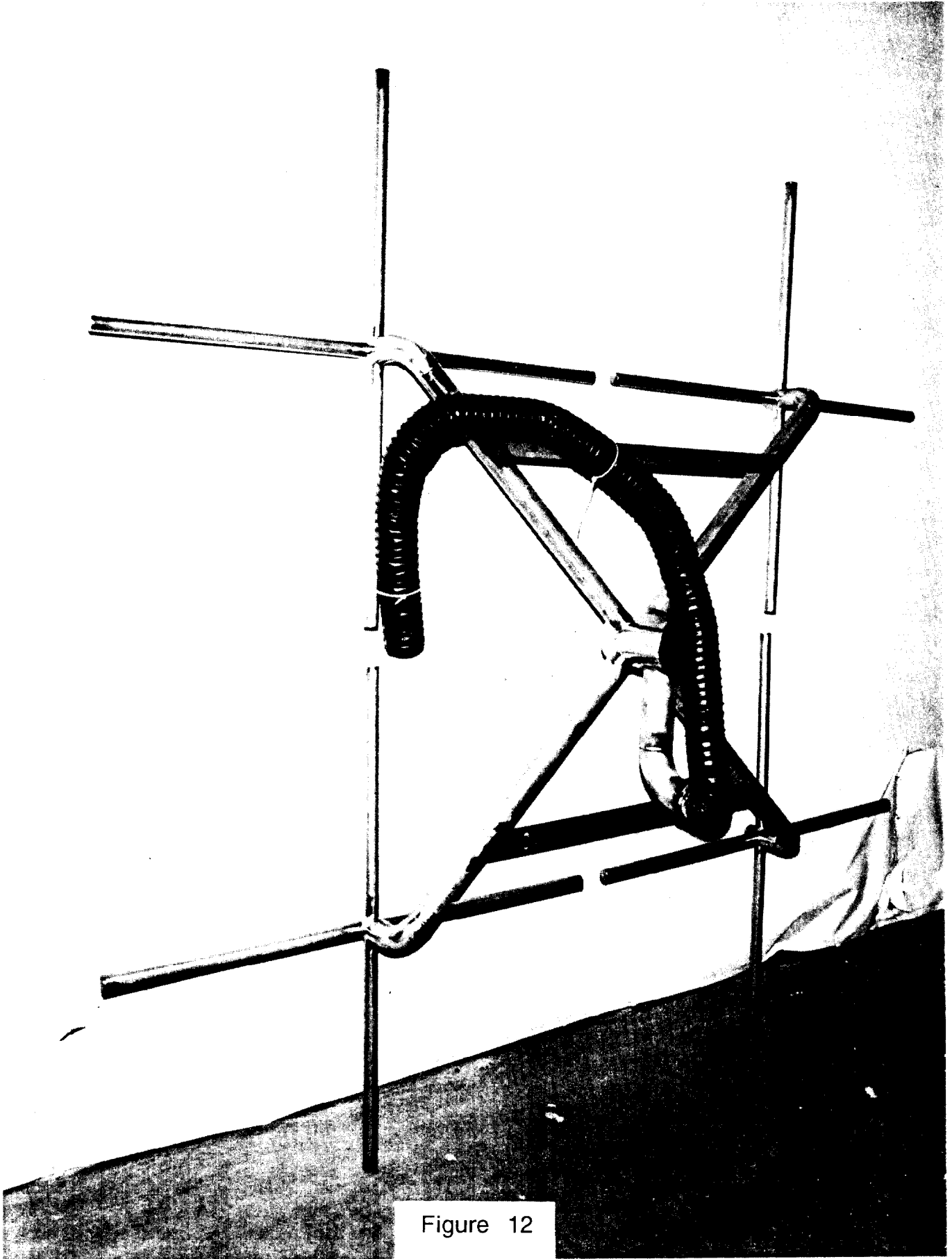


Figure 12

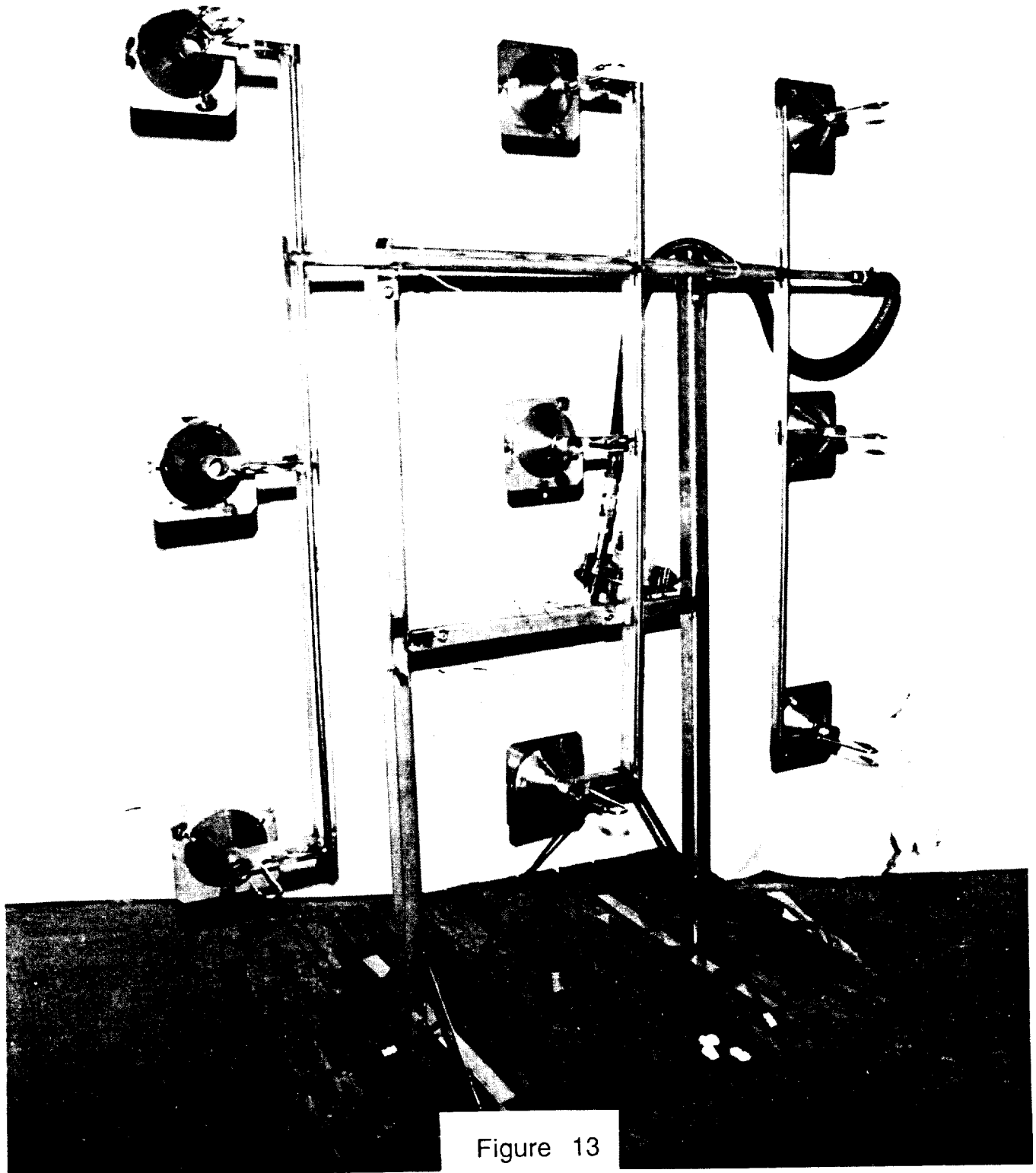


Figure 13

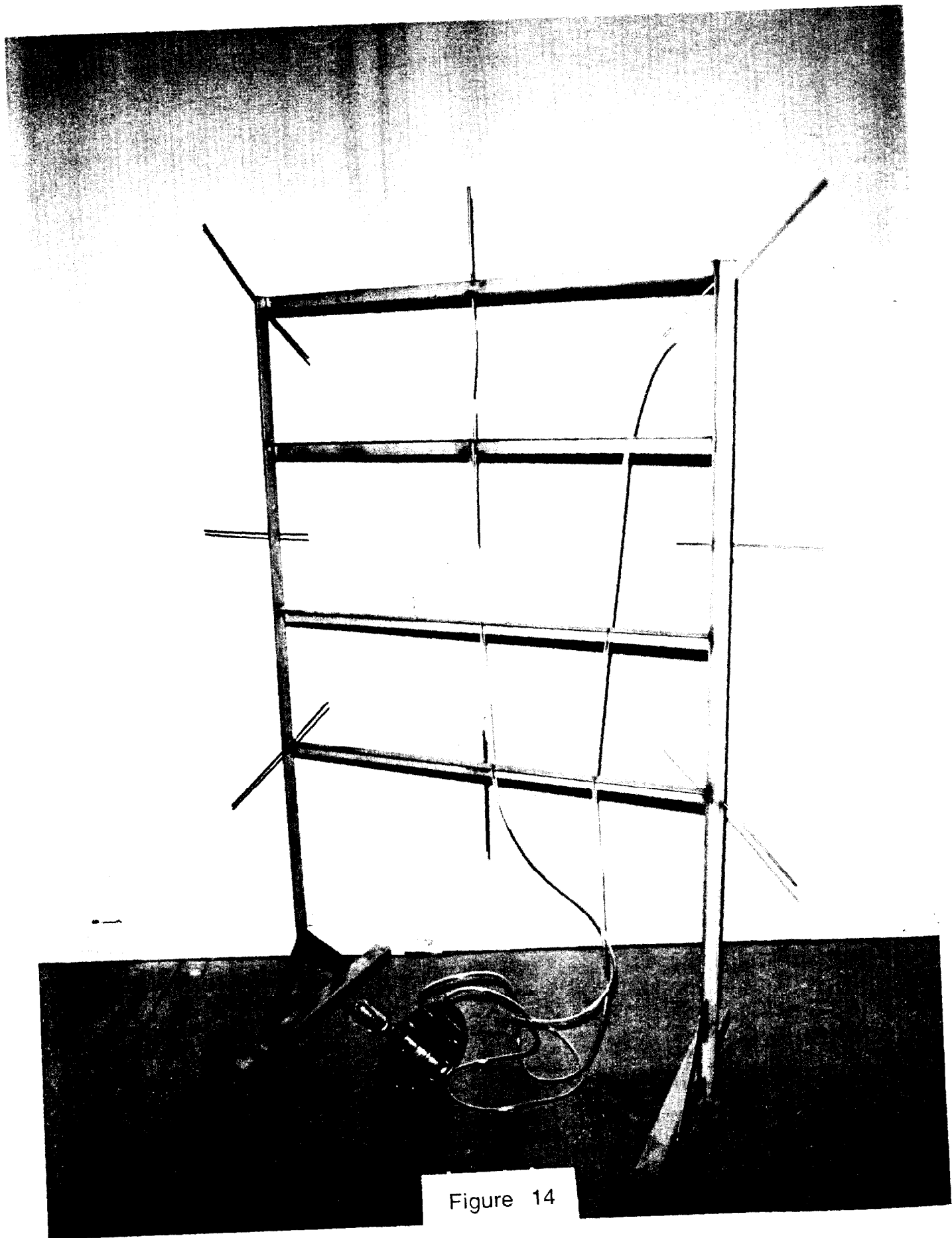


Figure 14



Figure 15

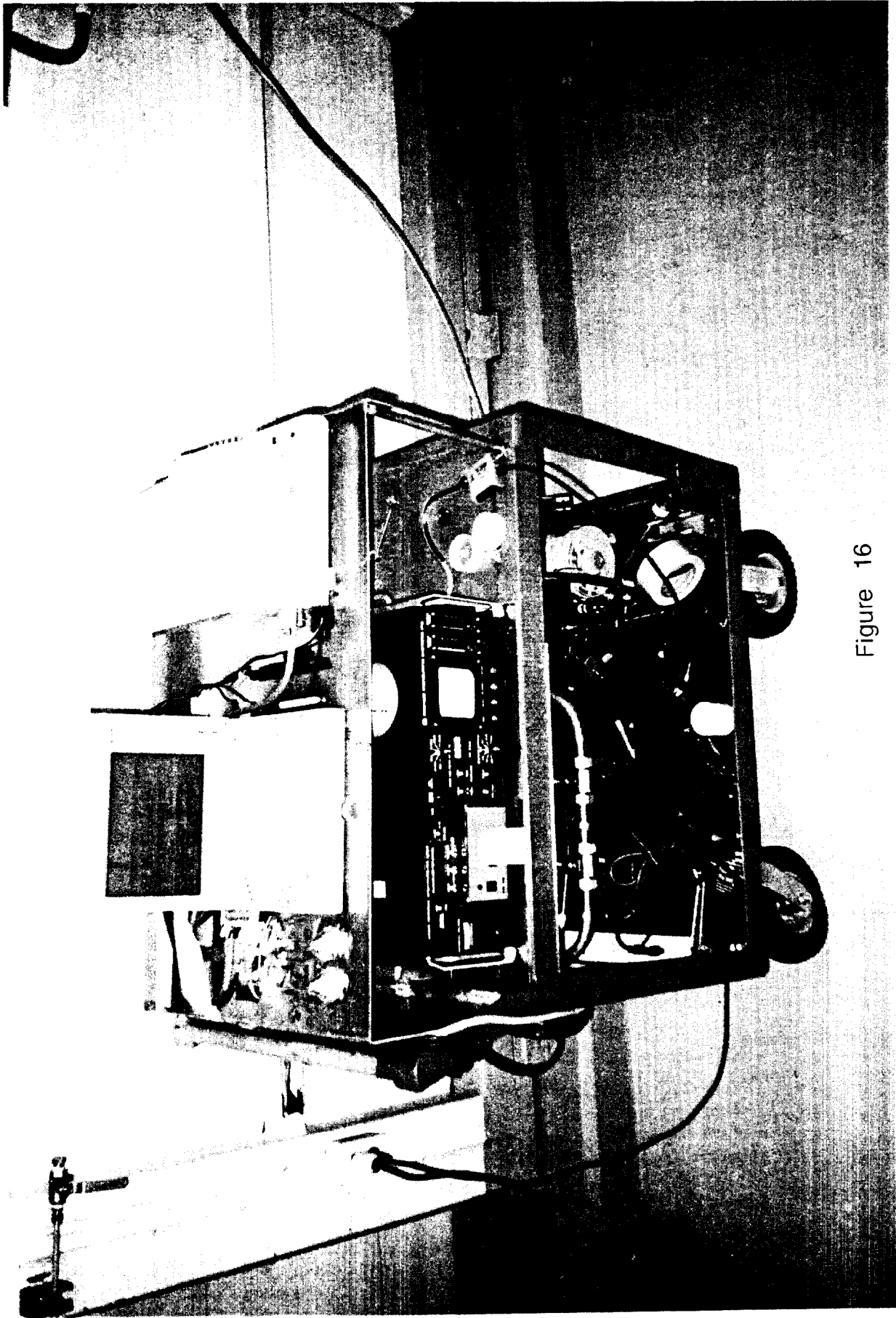


Figure 16

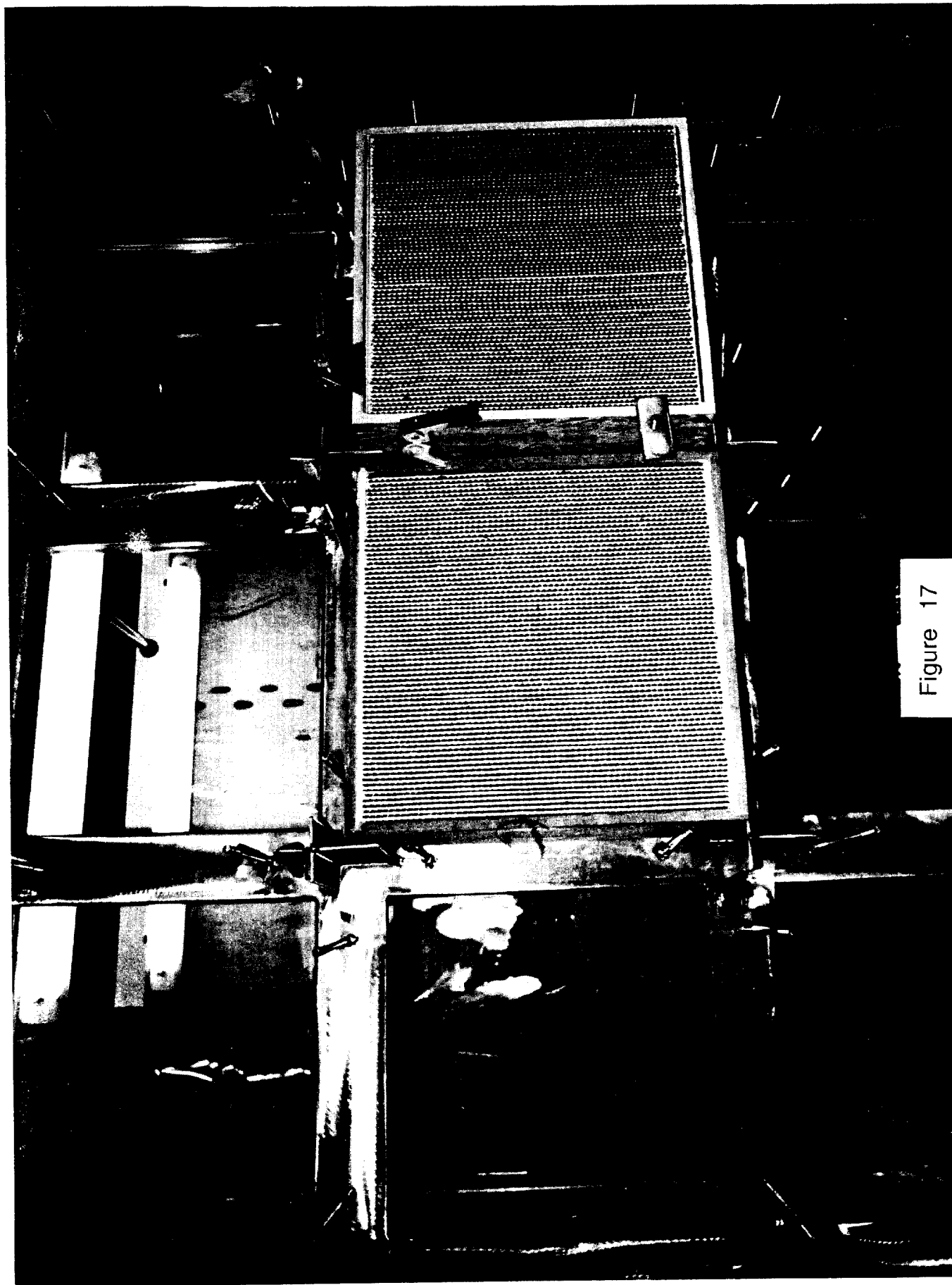


Figure 17

DISCUSSION

**FIRST:** You have described a very exciting project, and I look forward to hearing a full report at the next Air Cleaning Conference. I have a question regarding the selection of your equipment, did you build it according to the directions in N-509?

**FRETTHOLD:** These were manifolds that were already built to N-509 specifications and used in other plenums. We contacted a couple of manufacturers and asked them what they had that we could use. Better than trying to reinvent the wheel, we thought we could take what was already out there and analyze it for our use.

**FIRST:** I guess the diagrams are not as revealing as they might be, because as I looked at them I could not make the connection between what you showed and what is in N-509. But I am, indeed, very happy to learn that they were built according to N-509, because I think questions remain as to how good that design is in practice. Let me make one more comment, it concerns the matter you brought up of having one clamp holding two filters. I believe that is not approved according to the Nuclear Air Cleaning Handbook. How did it come about?

**FRETTHOLD:** I think most of these installations were built during the 50s and there were space restrictions. Engineering tried to cram everything they could into the smallest amount of space with no concern for service requirements. It was a learning process.

**FIRST:** I had the impression that you had rebuilt it, that is why I made the comment.

**JACOX:** First, when you bought these manifolds that had been built for some other application, did you get sufficient documentation to show how qualification was proven? Second, the way N-509 is written, the manifolds are system-specific, at least to a very large extent. So I think that part of your research ought to be to see that they are requalified properly. The design of a manifold for testing is as much an art as a science, so they are very specific to a particular type of housing and filter bank. I recommend that you look at this very carefully and also get what documentation you can from whomever you purchased them.

**FRETTHOLD:** I did ask for documentation and did receive it. I also had the design set up for our array of filters. It was arranged specifically for that plenum, with the idea that it would have the coverage needed. We will be verifying that we do indeed have the coverage needed and looking at which one will give us the best performance. This is a starting point. Then, we will specify modifications. As far as retrofitting other plenums, this one is a typical plenum. We have many approximately that size, with similar air flow patterns, entries, distance between demisters, distance between filter banks, etc. Therefore, we will be looking at the basic pattern, first of all. Then, when we retrofit existing plenums in the hot areas, we will go in, do air flow calculations, and cover all of the requirements. We will try to keep the work to a minimum, this is why we are starting out with something that looks like it will work.